

Integrated growth factor signaling promotes lung epithelial progenitor cell expansion and maintenance in mice and humans

Alyssa J. Miller^{1,2}, Briana R. Dye⁵, Melinda S. Nagy², Yu-Hwai Tsai², Sha Huang², Michael A.H. Ferguson², Jason R. Spence^{1,2,3,4*}

1. Program in Cellular and Molecular Biology

2. Department of Internal Medicine

3. Department of Cell and Developmental Biology

4. Center for Organogenesis

University of Michigan Medical School, Ann Arbor, Michigan 48109

5. Department of Biomedical Engineering

University of Michigan College of Engineering, Ann Arbor, Michigan 48109

* Author for correspondence:

Email: spencejr@umich.edu

ORCID: <http://orcid.org/0000-0001-7869-3992>

Author Contributions: AJM and JRS conceived the study and wrote the manuscript. AJM, BRD, YHT, MAHF and MSN conducted experiments. AJM, BRD, YHT, MAHF, MSN and JRS analyzed and interpreted results. AJM and JRS wrote the manuscript. All authors read, edited and approved the final content of the manuscript.

Conflicts of Interest: The authors have no conflicts to declare.

Abbreviations:

Bone Morphogenic Protein, BMP

Fibroblast Growth Factor, FGF

All-Trans Retinoic Acid, RA

Human Lung Organoid, HLO

Summary:

During lung branching morphogenesis, a multipotent progenitor population resides at the tips of bifurcating epithelial tubes that give rise to all lung epithelial cell types (1). Previously (2,3), we demonstrated that human pluripotent stem cells (hPSCs) could differentiate into human lung organoids (HLOs), which possessed airway-like structures and alveolar cells, but it was unclear if HLOs possessed a *bona fide* tip-progenitor population. The goal of the current study was to understand how tip-progenitors are regulated such that this population could be induced in HLO cultures. Using isolated embryonic mouse and human fetal tip-progenitors, we identified factors that promoted long-term growth and maintenance of this population *in vitro*. Our results showed significant functional and expression differences between mouse and human tip-progenitors, and demonstrated *de novo* induction of a robust population of budding, SOX9+ progenitor-like cells in HLOs.

Introduction:

During development, the lung undergoes branching morphogenesis, where a series of stereotyped epithelial bifurcations give rise to the branched, tree-like architecture of the adult lung (4). A population of rapidly proliferating progenitor cells resides at the distal tips of the epithelium throughout the branching process (1,5). Branching morphogenesis and maintenance of the distal tip progenitor cells is regulated by a series of complex mesenchymal-epithelial interactions that involve multiple signaling events, transcription factors, and dynamic regulation of the physical environment (6-13).

The molecular regulation of branching morphogenesis has been investigated in depth, with genetic mouse models playing a central role. These studies have identified major roles for several signaling events, including Wnt, Fibroblast Growth Factor (Fgf), Bone Morphogenic Protein (Bmp), Sonic Hedgehog (Shh), Retinoic Acid (RA) and Hippo signaling among others (14-36). These studies have shown the importance of epithelial-mesenchymal cross talk for regulating processes such as branching morphogenesis and proximal-distal patterning (6), and due to the complex and intertwined nature of these signaling networks, perturbations in one pathway affect signaling activity of others (9,10,37). This understanding of murine lung development has been used as a guide to direct differentiation of human pluripotent stem cells into lung lineages and 3-dimensional lung organoids (2,3,38-44).

Despite the wealth of information gained from murine studies, significant gaps in our understanding of lung development remain, especially in the context of human lung development. For example, it remains unknown how closely developmental processes in the murine lung mirror human lung development. Furthermore, due to the interdependence of mesenchymal and epithelial cell types, and the complex signaling events that interact to control this process, the precise mechanisms that control distal tip progenitor cell maintenance and cell fate differentiation have remained elusive.

These unknowns have been highlighted in our own studies that have attempted to differentiate lung lineages from hPSCs (2). For example, we have shown that hPSCs can be differentiated into human lung organoids (HLOs) that possess airway-like epithelial structures, but it is not clear if HLOs pass through distal-tip progenitor-like stage, mimicking the normal developmental events *in vivo*. This gap in knowledge also suggests that robustly predicting cellular outcomes during hPSC-differentiation is still a major challenge. This lack of predictive power may be due, in part, to species-specific differences between the mouse and human lung, to a poor understanding of human fetal lung development, or because the environment controlling the distal-tip progenitor cells is so complex.

The current work aimed to increase our understanding of how multiple growth factor signaling pathways interact to promote maintenance of distal epithelial progenitors in an undifferentiated state. Second, we aimed to elucidate the mechanisms by which distal epithelial progenitor cells of the human fetal lung are maintained in long-term culture. Third, we aimed to use new information gained from *ex vivo* culture of mouse and human fetal bud-tip progenitors in a predictive manner, in order to differentiate, *de novo*, distal epithelial lung progenitor-like cells from hPSCs.

Using isolated epithelial distal-tip progenitor cells from mouse and human fetal lungs during branching morphogenesis, we screened growth factors implicated in lung development individually and in combination for their ability to promote tissue expansion and maintenance of progenitor identity *in vitro*. Our results demonstrated that FGF7 promoted robust growth and expansion of both mouse and human epithelial progenitors, but could not maintain the progenitor population, which underwent differentiation. In the mouse, FGF signaling (FGF7 +/- FGF10) plus either CHIR-99021 (to stabilize β -catenin) or All-trans Retinoic Acid (RA) increased mRNA and protein expression of the distal epithelial progenitor marker, SOX9, and led to long-term growth and improved epithelial architecture *in vitro*. Synergistic activity of all 4 factors (FGF7/FGF10/CHIR-99021/RA; 4-factor; '4F' conditions) led to the highest mRNA expression of Sox9 in mice, whereas in human fetal lung buds we found that only 3-factors '3F' (FGF7, CHIR-99021, RA) were required to maintain long-term growth and expression of distal epithelial progenitor genes, including SOX9, ID2 and NMYC. Together, these results suggested that FGF, WNT and RA signaling act synergistically to maintain distal progenitor identity *in vitro* in both mouse and human distal-tip progenitor cells, but that these pathways affected epithelial progenitors in subtly different ways between species. Unexpectedly, our studies also revealed that distal epithelial progenitor cells in the human lung express SOX2, which is exclusively expressed in the proximal airway in mice (45,46), identifying an important molecular difference between mouse and human progenitor cells.

When applied to hPSC-derived foregut spheroid cultures, we observed that 3F conditions promoted robust epithelial growth into larger organoid structures. hPSC-derived organoids grown in 3F media developed a patterned epithelium, with proximal airway-like domains and distal epithelial bud-like domains that possessed SOX9/SOX2+ cells with a molecular profile similar to the human fetal lung buds. Taken together, these studies provide an improved mechanistic understanding of human lung epithelial progenitor cell regulation, and highlight the importance of using developing tissues to provide a framework for improving differentiation of hPSCs into specific lineages.

Results:

Isolation and in vitro culture of murine distal lung bud epithelium

During branching morphogenesis, the distal epithelial bud tips are comprised of progenitor cells that remain in the progenitor state until the branching program is complete (47) and will give rise to all the mature cell types of the lung epithelium (1). However, the mechanisms maintaining distal progenitors in an undifferentiated state remain unclear. This population of progenitor cells is known to express several transcription factors, including Sox9, Nmyc and Id2 (1,47-51). In order to study this population of cells, epithelial buds were mechanically isolated from lungs of embryonic day (E) 13.5 Sox9-eGFP mice and cultured in a Matrigel droplet (Figure 1A). Sox9-eGFP heterozygous lung bud tips were confirmed to have the same level of Sox9 mRNA as their wild type counterparts by QRT-PCR analysis (Figure 1- figure supplement 1A). The isolated Sox9+ population was confirmed by GFP expression (Figure 1B).

FGF7 promotes growth and expansion of distal epithelial lung buds

We sought to identify culture conditions that could support the long-term growth of distal epithelial buds in culture. We identified signaling events from the literature essential for normal mouse lung epithelial development, including FGF signaling (FGF7 and 10) (19,31,52-55); Wnt signaling (14,16,30,56-59); BMP signaling (17,60) and RA signaling (32,33,61,62). Many of these signaling events have previously been used for *in vitro* differentiation of hPSC-derived lung tissue (39-43,63-65). We performed a low-throughput screen to identify factors that could promote growth of distal bud tips in culture. The screen included FGF7, FGF10, BMP4, All Trans Retinoic Acid (hereafter referred to as 'RA') and CHIR-99021, which inhibits GSK3 β and stabilizes β -catenin (β CAT) leading to activation of β CAT-dependent signaling (Figure 1C). Treating buds with no growth factors (basal media, control) or individual growth factors showed that FGF7 promoted growth, expansion and survival of isolated buds for up to two weeks (Figure 1C). We also conducted an experiment in which all 5 factors (5F) were combined together, with one factor removed at a time (Figure 1D). Buds grew robustly in 5F media, whereas removing FGF7 from the 5F media (5F - FGF7) led to a loss of growth, even after 5 days in culture (Figure 1D). It was interesting to note that the same concentration of FGF7 and FGF10 did not have the same effect on lung bud outgrowth, since both ligands act on the FGF Receptor 2 (IIIb) isoform (FGFR2IIIb) (66,67), and both ligands are present in the lung during branching morphogenesis (19,21,68). Previous studies have offered evidence showing that FGF10 has structural similarities with FGF7, but is differentially regulated by components of the extracellular matrix, which may influence the ease of diffusion of the ligand (69). To test the possibility that diffusion of ligand through the matrix may explain experimental differences, we treated buds with a 50-fold excess of FGF10 (500ng/mL compared to 10ng/mL). A high concentration of FGF10 led to modest growth of buds and was sufficient

to keep buds alive in culture for up to 5 days, but cultures did not exhibit the same level of growth as those treated with low levels of FGF7 (Figure 1D).

Initial experimental conditions used FGF7 concentrations based on previous literature (10ng/mL; Figure 1) (39). We next tested if FGF7 affected growth in a concentration dependent manner by treating isolated buds with increasing concentrations of FGF7 and performing an EdU incorporation assay (Figure 1-figure supplement 1B-C). After one week in culture, cultures were pulsed with EdU for 1 hour prior to Fluorescence Activated Cell Sorting (FACS). Results showed that treating cultures with 50-100 ng/mL of FGF7 increased proliferation significantly above cultures that only received 1-10 ng/mL of FGF7 (Figure 1-figure supplement 1C). Despite this increase in proliferation, cultures at lower doses of FGF7 appeared qualitatively healthy (Figure 1-figure supplement 1B). Additionally, expansion of buds in 10ng/mL FGF7 was more robust than 1ng/mL, and cultures appeared less compact and dense compared to higher doses (Figure 1-figure supplement 1B). Based on these results, FGF7 was used at a concentration of 10 ng/mL for the remainder of our experiments.

FGF7 promotes growth of Sox9⁺ progenitors followed by cellular differentiation in long-term lung cultures.

In order to determine if FGF7 was promoting expansion of Sox9⁺ distal progenitors cells, we performed a lineage trace utilizing Sox9-Cre^{ER}; Rosa26^{Tomato} mice. Tamoxifen was given to timed pregnant dams at E12.5, and epithelial lung buds were isolated 24 hours later, at E13.5 (Figure 1-figure supplement 1E). Isolated distal buds that were lineage labeled were placed *in vitro* in basal media (control) or with FGF7. We observed that the Sox9-Cre^{ER}; Rosa26^{Tomato} lineage labeled population expanded over time (Figure 1-figure supplement 1F). After two weeks in culture, FGF7-treated bud cultures were dense and contained cells that stained positive for mature markers of both alveolar cell types (AEC1 - AQP5; AEC2 - SFTPB) and bronchiolar cell types (Clara cells – SCGB1A1; multi-ciliated cells - Acetylated Tubulin; basal stem cells – P63) although cells in culture were scattered throughout the tissue and appeared to lack spatial organization (Figure 1E). None of the cells observed after two weeks in culture were positive for both SFTPC and SCGB1A1, an expression pattern that has been shown to mark bronchioalveolar stem cells (Figure 1-figure supplement 1D)(70). Many of these cell types in culture had similar morphologies as cells found at postnatal day 0 of the *in vivo* mouse lung (Figure 1F). We examined the changes of differentiation marker expression over time using QRT-PCR and observed that the length of time in culture led to significant increases in mature alveolar markers *Aqp5* and *Sftpb*, as well as an upward trend in the expression of the club cell marker *Scgb1a1*. However, time in culture had a less dramatic effect on expression of proximal cell markers *Foxj1*, *p63*, and *Sox2*. The expression of the distal progenitor marker *Sox9* was significantly reduced after 3 days in culture and continued to go down as the time in culture increased (Figure 1H). Collectively, this data strongly suggests that FGF7 promoted an initial expansion

of Sox9⁺ distal epithelial progenitor cells that subsequently underwent differentiation with longer times in culture.

FGF7, CHIR-99021 and RA act synergistically to maintain the distal progenitor identity in mouse lung buds *in vitro*

Given that FGF7 promoted robust expansion of distal buds *in vitro*, but was also permissive for differentiation, we wanted to identify additional growth factors that interacted with FGF signaling to maintain the undifferentiated SOX9⁺ distal progenitor cell state *in vitro*. To do this, we returned to the strategy of using 5F media, and removed one additional growth factor at a time to examine the effect on growth, and expression of Sox9 and Sox2 as markers of distal progenitor and proximal airway cells, respectively. Removing any single factor (FGF10, CHIR-99021, RA or BMP4) from '5F' culture media did not affect the ability of isolated buds to expand (Figure 2A; 5F control condition presented in Figure 1D). QRT-PCR analysis of buds after 5 days in culture showed that removing BMP4 led to a statistically significant increase in Sox9 expression levels when compared to other culture conditions (Figure 2B), and led to gene expression levels that were closest in expression levels of freshly isolated wild type (WT) E13.5 lung buds (Figure 2B). Sox2 gene expression was generally low in freshly isolated E13.5 lung buds, and in all culture conditions after 5 days *in vitro* (Figure 2B). We also assessed markers for several genes expressed in differentiating cells (Figure 2-figure supplement 1A-B), and noted that the removal of BMP4 from the 5F media also resulted in a significant increase in *Sftpb*, and reduced expression in the proximal markers *p63*, *Foxj1* and *Scgb1a1* (Figure 2-figure supplement 1A-B). Collectively, this data suggested that removing BMP4 from the media was ideal for supporting an environment with low expression proximal airway markers and high Sox9.

We next screened combinations of the remaining factors to determine a minimal set that promoted tissue expansion while maintaining the identity of distal epithelial progenitor cells. All conditions included FGF7 (10 ng/mL) due to its ability to potently support proliferation and tissue expansion (Figure 1, Figure 1-figure supplement 1). FGF10 (10 ng/mL), CHIR-99021 (3 μ M) and RA (50 nM) were added in combination with FGF7 and the effect on growth, gene and protein expression was observed after two weeks in culture (Figure 2C-E). We found that all conditions supported robust growth (Figure 2C) and expression of Sox9, *Id2* and *Nmyc*, while maintaining low levels of Sox2 (Figure 2D). In support of this observation, lineage tracing experiments utilizing Sox9-Cre^{ER};Rosa26^{Tomato} mice, in which Tamoxifen was administered to timed pregnant dams at E12.5 and epithelial lung buds were isolated at E13.5, showed an expansion of labeled progenitors over the 2 week period in culture (Figure 2-figure supplement 1E). We noted that explanted buds treated with 4F or 3-Factor conditions ('3F'; FGF7, CHIR-99021, RA) maintained Sox9 mRNA expression at the highest levels, similar to those expressed in freshly isolated epithelial buds at E13.5 (Figure 2D). Additional QRT-PCR analysis of differentiation markers further suggested that 3F

and 4F conditions promoted optimal expression of distal progenitor identity markers while keeping proximal airway marker gene expression low (Figure 2-figure supplement 1C-D). Immunofluorescence and whole mount immunostaining of buds after 2 weeks in culture supported QRT-PCR data and showed that 3F and 4F conditions supported robust SOX9 protein expression (Figure 2E-F).

To determine if SOX9⁺ cells maintained in culture were multipotent and retained the ability to differentiate, we expanded isolated buds in 4F media for 5 days and then removed FGF10, CHIR-99021 and RA (retaining FGF7 only) for 4 days to determine if SOX9 protein/mRNA expression was reduced and if cells could differentiate (Figure 2-figure supplement 1F-J). Compared to controls, which received 4F media for the entire experiment, buds grown in FGF7 exhibited a reduction of SOX9 protein and mRNA expression (Figure 2-figure supplement 1G-H). We noted that many AQP5⁺ and SFTPC⁺ cells co-expressed SOX9 in 4F media, whereas tissue grown in FGF7 did not co-express SOX9, suggesting differentiation towards a more mature AECI or AECII-like cell (Figure 2-figure supplement 1H). These results suggested that SOX9⁺ cells maintained in culture retain the ability to down-regulate distal progenitor gene expression and undergo multi-lineage differentiation.

Long-term *in vitro* growth and maintenance of human fetal distal epithelial lung progenitors

Given that almost nothing is known about the functional regulation of human fetal distal lung epithelial progenitor cells, we asked if conditions that maintained mouse distal epithelial progenitors also supported human fetal distal lung progenitor growth and expansion *in vitro*. Distal epithelial lung buds were enzymatically and mechanically isolated from the lungs of 3 different biological samples at 12 weeks of gestation (84-87 days; n=3) and cultured in a Matrigel droplet (Figure 3A-B). Surprisingly, while characterizing the isolated buds, whole mount immunostaining revealed that human bud-tip epithelial progenitors express both SOX9 and SOX2 at 12 weeks (Figure 3C). This is in stark contrast to mice, where SOX9 is exclusively expressed in the distal lung-bud epithelium and SOX2 is exclusively expressed in the proximal airway epithelium(50,51). Further investigation of paraffin embedded fetal lungs ranging from 10-19 weeks of gestation revealed that SOX2/SOX9 double-positive cells are present in distal epithelial cells until about 14 weeks gestation (Figure 3D; Figure 3-figure supplement 1C). By 16 weeks, SOX9 and SOX2 became localized to the distal and proximal epithelium, respectively, and were separated by a SOX9/SOX2-negative transition zone, which continued to lengthen throughout development (Figure 3 - figure supplement 1C). Similar to isolated mouse lung bud cultures, we observed that FGF7 promoted robust growth *in vitro* after 2 and 4 weeks, but resulted in reduced growth after 6 weeks in culture (Figure 3E). However, all other groups tested permitted expansion and survival of buds in culture for 6 weeks or longer (Figure 3E). Human fetal buds exposed to 3F or 4F supported robust protein and mRNA expression of the distal progenitor markers SOX9, *ID2*

and *NMYC* (Figure 3F-H). In contrast, culture in only 2 factors (FGF7+CHIR-99021, or FGF7+RA) did not support robust distal progenitor marker expression (Figure 3F-H). Buds cultured in 3F or 4F media also had lower expression of the proximal airway markers *P63* and *SCGB1A1* (Figure 3-figure supplement 1A-B). In stark contrast to results in distal progenitors from mice, *SOX2* was also robustly expressed in the 3F and 4F conditions in human fetal buds (Figure 3H). Whole mount protein staining of *SOX2* and *SOX9* in buds treated with 3F media confirmed that almost all cells co-express *SOX2* and *SOX9*, similar to native human lung buds in fetal lungs younger than 16 weeks.

Our analysis demonstrated that 3F and 4F media functioned in a similar manner in human fetal buds, and suggested that the addition of FGF10 to the media did not have a significant effect on bud growth or differentiation. We further examined the effect of FGF10 on human fetal lung buds in culture by exposing them to high concentrations of FGF10 (500ng/mL). We observed that high concentrations of FGF10 induced only modest growth when compared to control conditions (basal media) (Figure 3-figure supplement 1D). On the other hand, the addition of a Rho-kinase inhibitor (Y27632) in combination with FGF10, but not alone, promoted growth of buds into larger cyst-like structures (Figure 3-figure supplement 1D). These results further support the notion that even at high concentrations, FGF10 alone does not have strong mitogenic effects on the human distal progenitor epithelium *in vitro*. Collectively, our data showed that a combination of FGF7, RA and activation of Wnt signaling (via CHIR-99021) is a minimal essential combination that promotes growth and maintain distal progenitor identity in long-term culture.

3F media induces a distal lung bud progenitor-like population of cells in hPSC-derived lung organoids.

Given the robustness by which 3F media supported mouse and human lung bud progenitor growth and identity, we sought to determine whether these culture conditions could promote a distal epithelial lung progenitor-like population from hPSCs. NKX2.1+ ventral foregut spheroids were generated as previously described(2,3), and were cultured in a droplet of Matrigel and overlaid with media containing 3F (FGF7, CHIR-99021, RA). Spheroids were considered to be “day 0” on the day they were placed in Matrigel. Organoids (called Human Lung Organoids; HLOs) grown in 3F media exhibited robust and stereotyped growth patterns and survived in culture for over 16 weeks (Figure 4A-B, Figure 4-figure supplement 1A-B). Epithelial structures grew first as cystic structures over the course of 2 weeks, followed by a period of epithelial folding that occurred between weeks 3-4 (Figure 4A and Figure 4-figure supplement 1C-D). Around 5-6 weeks in culture, the epithelial structures began forming bud-like structures that resembled human fetal epithelial distal bud tips that underwent bifurcations (Figure 4A-B, Figure 4-figure supplement 1D, bottom row). HLOs were passaged by gently removing Matrigel and replating in a fresh droplet while preserving structural integrity. In this way, HLOs were able to grow for over 16 weeks in

culture while retaining their original shape. HLOs could also be passaged using mechanical shear through a 27-gauge needle, followed by embedding in fresh Matrigel and 3F media (Figure 4-figure supplement 1E). Following passage, HLOs robustly re-established many small cysts that were expanded and serially passaged every 7-10 days many times (Figure 4-figure supplement 1F). The majority of HLO cysts formed from needle passaging were composed of cells with SOX2 and SOX9 nuclear co-staining (Figure 4-figure supplement 1G), suggesting that a population of SOX2/SOX9 double positive cells can be expanded easily in culture.

HLOs cultured in 3F media exhibited robust Nkx2.1 protein expression, a lung epithelial marker, in all cells (Figure 4C); however, it is worth noting that mRNA expression levels of Nkx2.1 were significantly lower than expression levels in the native human fetal lung (Figure 4-figure supplement 2E).

In addition to the cystic epithelial phenotype noted above, we also observed organoids that possessed a dense phenotype (Figure 4-figure supplement 2A-D). Dense organoids made up the majority of structures in FGF7-only growth conditions, whereas they made up about ~20% of cultures in 3F media. Approximately 35% of organoids in 3F media were made up of mixed structures (dense + epithelial) (Figure 4-figure supplement 2B). Dense structures consisted of cells expressing AECI cell markers HOPX and PDPN that were negative for ECAD (Figure 4-figure supplement 2C-D), consistent with adult human AECI cells(71). No staining for the mature AECII marker SFTPB was observed in dense structures (Figure 4-figure supplement 2C). Because we were most interested in studying the regulation of distal tip progenitor-like cells, we focused on epithelial organoids for the remainder of the analysis.

3F HLOs maintain regions of SOX9+/SOX2+ distal progenitor-like cells for over 115 days in culture and exhibit proximal-distal patterning

After 40 days in culture, 3F HLOs display clear proximal-distal patterning that mimics what is seen in the developing human lung. Small buds at the periphery of the HLOs stain positive for SOX2 and SOX9 (Figure 4D), similar to what is seen in the native human fetal lung during early branching (Figure 3D; Figure 3-figure supplement 1C), whereas interior regions of the HLOs are positive only for SOX2 staining (Figure 4D). SOX9+/SOX2+ peripheral regions persist until at least 115 days in culture (Figure 4E), although the bud regions become more cystic as the HLOs age past 8 weeks. QRT-PCR analysis confirmed that SOX2, *NMYC*, and *ID2* expression levels are not significantly different between the embryonic human lung and 54 day HLOs (Figure 4F) while the expression of mature markers are reduced in HLOs compared to human fetal lungs (Figure 4-figure supplement 2G-H). Similarly, QRT-PCR analysis of isolated human buds versus isolated bud regions from HLOs confirmed that HLO buds have a similar transcriptional profile to isolated 12-week human buds (Figure 4G).

Interior regions of 3F HLOs contain secretory cells

Interior regions of the HLOs showed protein staining for SCGB1A1, a marker of club cells, and MUC5AC, a marker of goblet cells, two prominent secretory cell types of the human proximal airway (Figure 4H-I). We also observed Acetylated-Tubulin (AcTub) accumulation on the apical surface of many cells, a marker of multiciliated cells (Figure 4H); however, these cells did not have *bona fide* cilia. We also observed the build-up of a dark, sticky substance within HLOs beginning around 6-7 weeks of culture (Figure 4A), and Periodic Acid Shift, Alcian Blue (PAS/AB) staining suggested that this was secreted mucous. Staining clearly shows cells within the HLOs that are positive for mucin, as well as secreted mucus in the lumen of HLOs, similar to what is seen in the adult human lung (Figure 4J).

Removal of CHIR-99021 and RA promotes differentiation within HLOs

Based on our results in the mouse showing that FGF7 was permissive for differentiation (Figure 1), we hypothesized that removing CHIR-99021 and RA from HLOs grown in 3F media would reduce the number of progenitor cells and increase differentiation of mature cell types within HLO cultures. Foregut spheroids were collected and grown in 3F media for 42 days and were cultured for an additional 26 days in 3F media (control) or media containing FGF7 only (Figure 5A). Morphologically, HLOs cultured in FGF7 lost the peripheral bud-like regions compared to 3F HLOs (Figure 5B). At the end of the experiment, cultures were collected and assessed for gene and protein expression. While 3F HLOs maintained budded peripheral regions containing cells with nuclear SOX9 and SOX2, HLOs grown in FGF7-only did not exhibit any SOX9/SOX2 double positive cells and instead contained regions with cells containing cytoplasmic SOX9 and separate regions where cells expressed nuclear SOX2 (Figure 5C). QRT-PCR analysis of SOX9 showed no change in the amount of SOX9 transcript, but a significant increase in SOX2 transcript in the FGF7 treated HLOs was observed (Figure 5D).

HLOs treated with FGF7 also exhibited an increase in many mature cell types as observed both by protein staining and QRT-PCR analysis. Most strikingly, FGF7-only HLOs exhibited a large increase in the number of MUC5AC positive cells, a dramatic increase the amount of mucous within the HLO lumens (Figure 5E), as well as a significant increase in gene expression of MUC5AC (Figure 5F). Interestingly, there was not an obvious increase in the number of SCGB1A1+ cells observed by protein staining (Figure 5I). Although expression levels of *SCGB1A1* were increased almost 100-fold in FGF7-only HLOs over the 3F controls, this difference was not statistically significant (Figure 5F). FGF7 treated HLOs also contained cells that stained positive for P63, a marker of basal stem cells (Figure 5G), and exhibited a significant increase in mRNA expression of *P63* (Figure 5H). In contrast, P63+ cells were conspicuously absent from 3F

epithelial HLOs. (Figure 5G-H, see also Figure 4H). Although mRNA expression of the proximal ciliated cell marker *FOXJ1* increased significantly in HLOs treated with FGF7-only (Figure 5O), obvious FOXJ1 protein expression was not detected by immunofluorescence (negative data not shown).

In addition to an increase expression of multiple proximal airway cell markers, HLOs grown in FGF7-only exhibited an increase in both protein and mRNA expression of the AECII marker *SFTPC* (Figure 5K-L) and possessed cells that stained positive for the AECl marker PDPN, and had increased gene expression of the AECl marker *HOPX*. (Figure 5M-N). Together, these results demonstrate that HLOs grown in 3F media have the ability to generate multiple mature lung cell lineages when CHIR-99021 and RA is removed from the media.

Discussion:

The ability to study human lung development, homeostasis and disease is limited by our ability to carry out functional experiments in human tissues. This has led to the development of many different *in vitro* model systems using primary human tissue, and using cells and tissues derived from hPSCs (72). Current approaches to differentiate hPSCs have used many techniques, including the stochastic differentiation of lung-specified cultures into many different cell types (39,63), FACS based sorting methods to purify lung progenitors from mixed cultures followed by subsequent differentiation (38,41,42), and by expanding 3-dimensional ventral foregut spheroids into lung organoids (2,3). During normal development, early lung progenitors transition through a SOX9+ distal progenitor cell state on their way to terminal differentiation, and it is assumed that in many hPSC-differentiation studies, NKX2.1-positive cells specified to the lung lineage also transition through a SOX9+ distal epithelial progenitor state prior to differentiating; however, this has not been shown definitively. For example, studies have identified methods to sort and purify Carboxypeptidase-M (CPM)-positive progenitor cells from a mixed population(41,42). However, whether or not this population represents a distal epithelial progenitor or is representative of an earlier stage lung progenitor is unknown. Moreover, the specific signaling networks that interact in order to induce and/or maintain this progenitor cell state are not well understood. The current study aimed to elucidate the signaling interactions that are required to maintain and expand the distal progenitor population in mouse and human fetal lungs, and to induce, expand and maintain a population of distal epithelial lung progenitor-like cells from hPSCs. Passing through a distal progenitor cell state is a critical aspect of normal lung epithelial development *en route* to becoming an alveolar or airway cell type (1), and so achieving this with hPSC-derived models is an important step toward faithfully modeling the full complement of developmental events that take place during lung organogenesis *in vivo*. Moreover, capturing this cell state *in vitro* will promote future studies aimed at understanding the precise mechanisms by which

progenitor cells make cell fate choices in order to differentiate into mature cell types.

Our study has identified a minimum core group of signaling pathways that synergize to efficiently support the maintenance of mouse and human distal progenitor cells cultured *ex vivo*, and have used the resulting information to differentiate distal lung progenitor-like cells from hPSCs. The robustness of the findings in mouse and human distal progenitors is highlighted by the ability to accurately predict how hPSCs will respond to 3F conditions. Using isolated embryonic tissue side-by-side with *in vitro* hPSC differentiation highlights the power of using the embryo as guide, but also shows the strength of hPSC-directed differentiation to confirm an observation. That is, if an experimental finding is truly biologically meaningful, the current work and past findings from others suggest that they can be used in a manner that predicts how a naïve cell will behave in the tissue culture dish (73-75). In this context, hPSCs and embryos can be viewed as complementary models that, when paired together, form a virtuous circle of discovery and validation.

Our studies also identified significant species-specific differences between the human and fetal mouse lung. Differences included both gene/protein expression differences, as well as functional differences when comparing how cells responded to diverse signaling environments *in vitro*. For example, SOX9 is exclusively expressed in the distal lung progenitors and SOX2 is exclusively expressed in the proximal airway in the developing mouse lung. In contrast, the distal progenitors in the human fetal lung robustly express both SOX2 and SOX9 until around 16 weeks of gestation. Others have noted similar differences with regards to expression Hedgehog signaling machinery (76). These mouse-human differences highlight the importance of validating observations made in hPSC-derived tissues by making direct comparisons with human tissues, as predictions or conclusions about human cell behavior based on results generated from the developing mouse lung may be misleading.

Our experimental findings, in combination with previously published work have also raised new questions, which may point to interesting avenues for future studies. Previously, we have shown that HLOs grown in high concentrations of FGF10 predominantly give rise to airway-like tissues, with a small number of alveolar cell types and a lack of alveolar structure (2,3). Here, our results suggest that high concentrations of FGF10 alone do not play a major role in supporting robust growth of human fetal lung buds. When comparing our previously published work and our current work, we also note that HLOs grown in high FGF10 possess abundant P63+ basal-like cells (2), whereas HLOs grown in 3F media lack this population. Similarly, HLOs grown in high-FGF10 lacked secretory cells (2), whereas we find evidence for robust differentiation of club and goblet cells in HLOs grown in 3F media. This data suggests that FGF10 may have different functional roles in the human fetal lung or that there are still unappreciated roles for FGF10 during lung morphogenesis, and also suggest

that we still do not fully appreciate how these signaling pathways interact to control cell fate decisions. Collectively, these observations lay the groundwork for future studies.

Taken together, our current work has identified that multiple signals are integrated into a network that is critical for long-term *in vitro* expansion and maintenance of mouse and human distal lung epithelial progenitors, and we have utilized this information to generate and expand, *de novo*, a population of distal lung epithelial progenitor-like cells from hPSCs. These conditions maintained progenitor-like cells in HLOs for over 115 days in culture, and generated HLOs that patterned, underwent stereotyped complex epithelial budding, and contained mature secretory cells. We believe this predictive approach will be a valuable tool to more carefully understand how certain environments control the differentiation of hPSCs, and that the HLOs described here can be used broadly to study human lung development, homeostasis and disease.

Methods:

Isolation and culture of mouse lung epithelial buds

All animal research was approved by the University of Michigan Committee on Use and Care of Animals. Lungs from Sox9-eGFP (MGI ID:3844824), Sox9CreER;Rosa^{Tomato/Tomato} (MGI ID:5009223 and 3809523)(77), or wild type lungs from CD1 embryos (Charles River) were dissected at embryonic day (E) 13.5, and buds were isolated as previously described (78). For experiments using Sox9CreER;Rosa^{Tomato/Tomato} mice, 50 ug/g of tamoxifen was dissolved in corn oil and given by oral gavage on E12.5, 24 hours prior to dissection.

Isolation and culture of human fetal lung epithelial buds

All research utilizing human fetal tissue was approved by the University of Michigan institutional review board. Normal human fetal lungs were obtained from the University of Washington Laboratory of Developmental Biology. Distal regions of 12 week fetal lungs were cut into ~2mm sections and isolate as described above.

EdU quantification by Flow Cytometry

Epithelial lung buds were dissected from e13.5 CD1 mice and plated in a matrigel droplet as described above. 3-4 individual buds from one mouse were placed in each droplet and were pooled to serve as a single biological replicate. Three droplets (corresponding to 3 independent biological samples) were assigned to each experimental group, receiving either 1, 10, 50 or 100 ng/mL of FGF7 for 7 days. Media was changed every 2-3 days. Cells were incubated with EdU for 1 hour and stained with the Click-It EdU Alexa Fluor 488 system (ThermoFisher Cat# C10337) according to the manufacturer's instructions. As a control, wells that received 10 ng/mL of FGF7 for 7 days were taken through the EdU steps but were not stained were used to set the gates. For analysis, lung buds were broken into a single cell suspension. 1mL of accutase (Sigma Cat#

A6964) was added to a 15mL conical tube containing pooled epithelial buds and cells were incubated at 37 degrees Celsius with frequent visual inspection until clumps of cells were no longer visible. 3mL of basal media (see below) was added to each tube, and cells were centrifuged at 300g for 5 minutes at 4 degrees Celsius. The supernatant was then withdrawn, and cells were resuspended with 1 mL sterile PBS, filtered through a 70 μ M strainer to remove any cell clumps and transferred to a cell sorting tube. Flow cytometric analysis was performed on a BD FACSARIA III cell sorter (BD biosciences).

Generation and culture of hPSC-derived lung organoids

The University of Michigan Human Pluripotent Stem Cell Research Oversight (hPSCRO) Committee approved all experiments using human embryonic stem cell (hESC) lines. hESC line UM63-1 (NIH registry #0277) was obtained from the University of Michigan and hESC line H9 (NIH registry #0062) was obtained from the WiCell Research Institute. ES cell lines were routinely karyotyped to ensure normal karyotype and ensure the sex of each line (H9 - XX, UM63-1 - XX). Cells are monitored for mycoplasma infection monthly using the MycoAlert Mycoplasma Detection Kit (Lonza). Stem cells were maintained on hESC-qualified Matrigel (Corning Cat# 354277) using mTesR1 medium (Stem Cell Technologies). hESCs were maintained and passaged as previously described (74) and ventral foregut spheroids were generated as previously described (2,3). Following differentiation, free-floating foregut spheroids were collected from differentiated stem cell cultures and plated in a matrigel droplet on a 24-well tissue culture grade plate.

Culture media, growth factors and small molecules

Growth factors and small molecules

Recombinant Human Fibroblast Growth Factor 7 (FGF7) was obtained from R&D systems (R&D #251-KG/CF) and used at a concentration of 10 ng/mL unless otherwise noted. Recombinant Human Fibroblast Growth Factor 10 (FGF10) was obtained either from R&D systems (R&D #345-FG) or generated in house (see below), and used at a concentration of 10 ng/mL (low) or 500 ng/mL (high) unless otherwise noted. Recombinant Human Bone Morphogenic Protein 4 (BMP4) was purchased from R&D systems (R&D Catalog # 314-BP) and used at a concentration of 10 ng/mL. All-trans Retinoic Acid (RA) was obtained from Stemgent (Stemgent Catalog# 04-0021) and used at a concentration of 50 nM. CHIR-99021, a GSK3 β inhibitor that stabilizes β -CATENIN, was obtained from STEM CELL technologies (STEM CELL Technologies Catalog# 72054) and used at a concentration of 3 μ M. Y27632, a ROCK inhibitor (APEX BIO Cat# A3008) was used at a concentration of 10 μ M.

Generation and Isolation of human recombinant FGF10

Recombinant human FGF10 was produced in-house. The recombinant human FGF10 (rhFGF10) expression plasmid pET21d-FGF10 in *E. coli* strain BL21(DE3) was a gift from James A. Bassuk at the University of Washington School of Medicine(79). *E. coli* strain was grown in standard LB media with

peptone derived from meat, carbenicillin and glucose. rhFGF10 expression was induced by addition of isopropyl-1-thio- β -D-galactopyranoside (IPTG). rhFGF10 was purified by using a HiTrap-Heparin HP column (GE Healthcare, 17040601) with step gradients of 0.5M to 2M LiCl. From a 200 ml culture, 3 mg of at least 98% pure rFGF-10 (evaluated by SDS-PAGE stained with Coomassie Blue R-250) was purified. rFGF10 was compared to commercially purchased human FGF10 (R&D Systems) to test/validate activity based on the ability to phosphorylate ERK1/2 in an A549 alveolar epithelial cell line (ATCC Cat#CCL-185) as assessed by western blot analysis.

RNA extraction and quantitative RT-PCR analysis

RNA was extracted using the MagMAX-96 Total RNA Isolation System (Life Technologies). RNA quality and concentration was determined on a Nanodrop 2000 spectrophotometer (Thermo Scientific). 100 ng of RNA was used to generate a cDNA library using the SuperScript VILO cDNA master mix kit (Invitrogen) according to manufacturer's instructions. qRT-PCR analysis was conducted using Quantitect SYBR Green Master Mix (Qiagen) on a Step One Plus Real-Time PCR system (Life Technologies). Expression was calculated as a change relative to GAPDH expression using arbitrary units, which were calculated by the following equation: $2^{-(\text{GAPDH Ct} - \text{Gene Ct})} \times 10,000$. A Ct value of 40 or greater was considered not detectable. A list of primer sequences used can be found in Table 1.

Statistical Analysis

All plots and statistical analysis was done using Prism 6 Software (GraphPad Software, Inc.). For statistical analysis of qRT-PCR results, at least 3 biological replicates for each experimental group were analyzed and plotted with the standard error of the mean. If only two groups were being compared, a two-sided student's T-test was performed. In assessing the effect of length of culture with FGF7 on gene expression in mouse buds (Figure 1G), a one-way, unpaired Analysis of Variance (ANOVA) was performed for each individual gene over time. The mean of each time point was compared to the mean of the expression level for that gene at day 0 of culture. If more than two groups were being compared within a single experiment, an unpaired one-way analysis of variance was performed followed by Tukey's multiple comparison test to compare the mean of each group to the mean of every other group within the experiment.

Tissue preparation, Immunohistochemistry and imaging

Paraffin sectioning and staining

Mouse bud, human bud, and HLO tissue was fixed in 4% Paraformaldehyde (Sigma) for 2 hours and rinsed in PBS overnight. Tissue was dehydrated in an alcohol series, with 30 minutes each in 25%, 50%, 75% Methanol:PBS/0.05% Tween-20, followed by 100% Methanol, and then 100% Ethanol. Tissue was processed into paraffin using an automated tissue processor (Leica ASP300).

Paraffin blocks were sectioned 5-7 μ m thick, and immunohistochemical staining was performed as previously described (80). A list of antibodies, antibody information and concentrations used can be found in Table 2. PAS Alcian blue staining was performed using the Newcomer supply Alcian Blue/PAS Stain kit (Newcomer Supply, Inc.) according to manufacturer's instructions.

Whole mount staining

For whole mount staining tissue was placed in a 1.5mL eppendorf tube and fixed in 4% paraformaldehyde (Sigma) for 30 minutes. Tissue was then washed with PBS/0.05% Tween-20 (Sigma) for 5 hours, followed by a 2.5-hour incubation with blocking serum (PBS-Tween-20 plus 5% normal donkey serum). Primary antibodies were added to blocking serum and tissue was incubated for at least 24 hours at 4 degrees Celcius. Tissue was then washed for 5 hours with several changes of fresh PBS-Tween-20. Secondary antibodies were added to fresh blocking solution and tissue was incubated for 12-24 hours, followed by 5 hours of PBS-Tween-20 washes. Tissue was then dehydrated to 100% methanol and carefully moved to the center of a single-well EISCO concave microscope slide (ThermoFisher Cat# S99368) using a glass transfer pipette. 5-7 drops of Murray's clear (2 parts Benzyl alcohol, 1 part Benzyl benzoate [Sigma]) were added to the center of the slide, and slides were coverslipped and sealed with clear nail polish.

Imaging and image processing

Images of fluorescently stained slides were taken on a Nikon A-1 confocal microscope. When comparing groups within a single experiment, exposure times and laser power were kept consistent across all images. All Z-stack imaging was done on a Nikon A-1 confocal microscope and Z-stacks were 3-D rendered using Imaris software. Brightness and contrast adjustments were carried out using Adobe Photoshop Creative Suite 6 and adjustments were made uniformly among all images.

Brightfield images of live cultures were taken using an Olympus S2X16 dissecting microscope. Image brightness and contrast was enhanced equally for all images within a single experiment using Adobe Photoshop. Images were cropped where noted in figure legends to remove blank space surrounding buds or cultures. Brightfield images of Alcian Blue stains were taken using an Olympus DP72 inverted microscope.

TABLE 1: qRT-PCR primer sequences

Species	Gene Target	Forward Primer Sequence	Reverse Primer Sequence
Mouse	aqp5	TAGAAGATGGCTCGGAGCAG	CTGGGACCTGTGAGTGGTG
Mouse	foxj1	TGTTCAAGGACAGGTTGTGG	GATCACTCTGTCTGGCCATCT
Mouse	gapdh	TGTCAGCAATGCATCCTGCA	CCGTTCTAGCTCTGGGATGAC
Mouse	id2	AGAAAAGAAAAAGTCCCCAAATG	GTCCTTGCAGGCATCTGAAT
Mouse	nmyc	AGCACCTCCGGAGAGGATA	TCTCTACGGTGACCACATCG
Mouse	p63	AGCTTCTTCAGTTCGGTGGG	CCTCCAACACAGATTACCCG
Mouse	Scgb1a1	ACTTGAAGAAATCCTGGGCA	CAAAGCCTCCAACCTCTACC
Mouse	sftp-b	ACAGCCAGCACACCCTTG	TTCTCTGAGCAACAGCTCCC
Mouse	sox2	AAAGCGTTAATTTGGATGGG	ACAAGAGAATTGGGAGGGGT
Mouse	sox9	TCCACGAAGGGTCTCTTCTC	AGGAAGCTGGCAGACCAGTA
Human	Foxj1	CAACTTCTGCTACTTCCGCC	CGAGGCACTTTGATGAAGC
Human	gapdh	AATGAAGGGGTCATTGATGG	AAGGTGAAGGTCGGAGTCAA
Human	hopx	GCCTTTCCGAGGAGGAGAC	TCTGTGACGGATCTGCACTC
Human	id2	GACAGCAAAGCACTGTGTGG	TCAGCACTTAAAAGATTCCGTG
Human	muc5ac*	GCACCAACGACAGGAAGGATGAG	CACGTTCCAGAGCCGGACAT
Human	nkx2.1	CTCATGTTTCATGCCGCTC	GACACCATGAGGAACAGCG
Human	nmyc	CACAGTGACCACGTCGATTT	CACAAGGCCCTCAGTACCTC
Human	p63	CCACAGTACACGAACCTGGG	CCGTTCTGAATCTGCTGGTCC
Human	scgb1a1	ATGAAACTCGCTGTCACCCT	GTTTCGATGACACGCTGAAA
Human	sftp-b	CAGCACTTTAAAGGACGGTGT	GGGTGTGTGGGACCATGT
Human	sox2	GCTTAGCCTCGTCGATGAAC	AACCCCAAGATGCACAACCTC
Human	sox9	GTACCCGCACTTGCAACAAC	ATTCCACTTTGCGTTCAAGG
Human	sp-c	AGCAAAGAGGTCCTGATGGA	CGATAAGAAGGCGTTTCAGG

Note: All primer sequences were obtained from <http://primerdepot.nci.nih.gov> (human) or <http://mouseprimerdepot.nci.nih.gov> (mouse) unless otherwise noted. All annealing temperatures are near 60°C.

*MUC5AC Huang, SX et al. Efficient generation of lung and airway epithelial cells from human pluripotent stem cells. Nature Biotechnol. 1–11 (2013). doi:10.1038/nbt.2754

Table 2: Antibody information

Primary Antibody	Source	Catalog #	Used for Species	Dilution (Sections)	Dilution (Whole mount)	Clone
Goat anti-CC10 (SCGB1A1)	Santa Cruz Biotechnology	sc-9770	Mouse, Human	1:200		C-20
Goat anti-SOX2	Santa Cruz Biotechnology	Sc-17320	Mouse, Human	1:200	1:100	polyclonal
Mouse anti-Acetylated Tubulin (ACTTUB)	Sigma-Aldrich	T7451	Mouse, Human	1:1000		6-11B-1
Mouse anti-E-Cadherin (ECAD)	BD Transduction Laboratories	610181	Mouse, Human	1:500		36/E-Cadherin
Mouse anti-Surfactant Protein B (SP-B)	Seven Hills Bioreagents	Wmab-1B9	Mouse, Human	1:250		monoclonal
Rabbit anti-Aquaporin 5 (Aqp5)	Abcam	Ab78486	Mouse	1:500		polyclonal
Rabbit anti-Clara Cell Secretory Protein (CCSP; SCGB1A1)	Seven Hills Bioreagents	Wrab-3950	Mouse, Human	1:250		polyclonal
Rabbit anti-HOPX	Santa Cruz Biotechnology	Sc-30216	Human	1:250		polyclonal
Rabbit anti-NKX2.1	Abcam	ab76013	Human	1:200		EP1584Y
Rabbit anti-PDPN	Santa Cruz Biotechnology	Sc-134482	Human	1:500		polyclonal
Rabbit anti-Pro-Surfactant protein C (Pro-SPC)	Seven Hills Bioreagents	Wrab-9337	Human, Mouse	1:500		polyclonal
Rabbit anti-P63	Santa Cruz Biotechnology	sc-8344	Mouse, Human	1:200		H-129
Rabbit anti-SOX9	Millipore	AB5535	Mouse, Human	1:500	1:250	polyclonal
Rat anti-Ki67	Biolegend	652402	Mouse	1:100		16A8
*Biotin-Mouse anti MUC5AC	Abcam	ab79082	Human	1:500		Monoclonal
Secondary Antibody	Source	Catalog #		Dilution		
Donkey anti-goat 488	Jackson Immuno	705-545-147		1:500		
Donkey anti-goat 647	Jackson Immuno	705-605-147		1:500		
Donkey anti-goat Cy3	Jackson Immuno	705-165-147		1:500		
Donkey anti-mouse 488	Jackson Immuno	715-545-150		1:500		
Donkey anti-mouse 647	Jackson Immuno	415-605-350		1:500		
Donkey anti-mouse Cy3	Jackson Immuno	715-165-150		1:500		
Donkey anti-rabbit 488	Jackson Immuno	711-545-152		1:500		
Donkey anti-rabbit 647	Jackson Immuno	711-605-152		1:500		
Donkey anti-rabbit Cy3	Jackson Immuno	711-165-102		1:500		
Donkey anti-goat 488	Jackson Immuno	705-545-147		1:500		
Donkey anti-goat 647	Jackson Immuno	705-605-147		1:500		
Donkey anti-goat Cy3	Jackson Immuno	705-165-147		1:500		
Donkey anti-mouse 488	Jackson Immuno	715-545-150		1:500		
Donkey anti-mouse 647	Jackson Immuno	415-605-350		1:500		

Donkey anti-mouse Cy3	Jackson Immuno	715-165-150		1:500		
Donkey anti-rabbit 488	Jackson Immuno	711-545-152		1:500		
Donkey anti-rabbit 647	Jackson Immuno	711-605-152		1:500		
Donkey anti-rabbit Cy3	Jackson Immuno	711-165-102		1:500		
Streptavidin 488	Jackson Immuno	016-540-084		1:500		

References:

1. Rawlins EL, Clark CP, Xue Y, Hogan BLM. The Id2+ distal tip lung epithelium contains individual multipotent embryonic progenitor cells. *Development*. 2009 Nov;136(22):3741–5. PMCID: PMC2766341
2. Dye BR, Hill DR, Ferguson MA, Tsai Y-H, Nagy MS, Dyal R, et al. In vitro generation of human pluripotent stem cell derived lung organoids. *Elife*. 2015;4. PMCID: PMC4370217
3. Dye BR, Dedhia PH, Miller AJ, Nagy MS, White ES, Shea LD, et al. A bioengineered niche promotes in vivo engraftment and maturation of pluripotent stem cell derived human lung organoids. *Elife*. eLife Sciences Publications Limited; 2016 Sep 28;5:e19732. PMCID: PMC5089859
4. Metzger RJ, Klein OD, Martin GR, Krasnow MA. The branching programme of mouse lung development. *Nature*. 2008 Jun 5;453(7196):745–50. PMCID: PMC2892995
5. Branchfield K, Li R, Lungova V, Verheyden JM, McCulley D, Sun X. A three-dimensional study of alveologenesis in mouse lung. *Developmental Biology*. 2015 Nov 26. PMCID: PMC4843524
6. Morrissey EE, Hogan BLM. Preparing for the First Breath: Genetic and Cellular Mechanisms in Lung Development. *Developmental Cell*. Elsevier Inc; 2010 Jan 19;18(1):8–23. PMCID: PMC3736813
7. Rock JR, Hogan BLM. Epithelial Progenitor Cells in Lung Development, Maintenance, Repair, and Disease. *Annu. Rev. Cell Dev. Biol.* 2011 Nov 10;27(1):493–512.
8. Domyan ET, Sun X. Patterning and plasticity in development of the respiratory lineage. *Dev. Dyn.* 2010 Dec 7;240(3):477–85. PMCID: PMC3103759
9. Hines EA, Sun X. Tissue crosstalk in lung development. *J Cell Biochem.* 2014 Sep;115(9):1469–77.
10. Morrissey EE, Cardoso WV, Lane RH, Rabinovitch M, Abman SH, Ai X, et al. Molecular determinants of lung development. *Ann Am Thorac Soc*. 2013

Apr;10(2):S12–6. PMCID: PMC3955361

11. Rawlins EL. The building blocks of mammalian lung development. *Dev. Dyn.* 2010 Nov 18;240(3):463–76.
12. Kim HY, Nelson CM. Extracellular matrix and cytoskeletal dynamics during branching morphogenesis. *Organogenesis.* 2012 Apr;8(2):56–64. PMCID: PMC3429513
13. Varner VD, Nelson CM. Cellular and physical mechanisms of branching morphogenesis. *Development.* Oxford University Press for The Company of Biologists Limited; 2014 Jul;141(14):2750–9. PMCID: PMC4197615
14. Shu W, Guttentag S, Wang Z, Andl T, Ballard P, Lu MM, et al. Wnt/beta-catenin signaling acts upstream of N-myc, BMP4, and FGF signaling to regulate proximal-distal patterning in the lung. *Dev Biol.* 2005 Jul 1;283(1):226–39.
15. Cornett B, Snowball J, Varisco BM, Lang R, Whitsett J, Sinner D. Wntless is required for peripheral lung differentiation and pulmonary vascular development. *Developmental Biology.* 2013 Jul 1;379(1):38–52. PMCID: PMC3699333
16. Goss AM, Tian Y, Tsukiyama T, Cohen ED, Zhou D, Lu MM, et al. Wnt2/2b and β -Catenin Signaling Are Necessary and Sufficient to Specify Lung Progenitors in the Foregut. *Developmental Cell.* Elsevier Ltd; 2009 Aug 18;17(2):290–8. PMCID: PMC2763331
17. Weaver M, Dunn NR, Hogan BL. Bmp4 and Fgf10 play opposing roles during lung bud morphogenesis. *Development.* 2000 Jun;127(12):2695–704.
18. Bellusci S, Henderson R, Winnier G, Oikawa T, Hogan BL. Evidence from normal expression and targeted misexpression that bone morphogenetic protein (Bmp-4) plays a role in mouse embryonic lung morphogenesis. *Development.* 1996 Jun;122(6):1693–702.
19. Bellusci S, Grindley J, Emoto H, Itoh N, Hogan BL. Fibroblast growth factor 10 (FGF10) and branching morphogenesis in the embryonic mouse lung. *Development.* 1997 Dec;124(23):4867–78.
20. Bellusci S, Furuta Y, Rush MG, Henderson R, Winnier G, Hogan BL. Involvement of Sonic hedgehog (Shh) in mouse embryonic lung growth and morphogenesis. *Development.* 1997 Jan;124(1):53–63.
21. White AC, Xu J, Yin Y, Smith C, Schmid G, Ornitz DM. FGF9 and SHH signaling coordinate lung growth and development through regulation of distinct mesenchymal domains. *Development.* 2006 Apr;133(8):1507–17.

22. Motoyama J, Liu J, Mo R, Ding Q, Post M, Hui CC. Essential function of Gli2 and Gli3 in the formation of lung, trachea and oesophagus. *Nat Genet.* 1998 Sep;20(1):54–7.
23. Yin Y, Wang F, Ornitz DM. Mesothelial- and epithelial-derived FGF9 have distinct functions in the regulation of lung development. *Development.* 2011 Aug;138(15):3169–77. PMCID: PMC3188607
24. Yin Y, White AC, Huh S-H, Hilton MJ, Kanazawa H, Long F, et al. An FGF–WNT gene regulatory network controls lung mesenchyme development. *Developmental Biology.* 2008 Jul;319(2):426–36. PMCID: PMC2757945
25. Domyan ET, Ferretti E, Throckmorton K, Mishina Y, Nicolis SK, Sun X. Signaling through BMP receptors promotes respiratory identity in the foregut via repression of Sox2. *Development. The Company of Biologists Limited;* 2011 Mar;138(5):971–81. PMCID: PMC4074297
26. Lu BC, Cebrian C, Chi X, Kuure S, Kuo R, Bates CM, et al. Etv4 and Etv5 are required downstream of GDNF and Ret for kidney branching morphogenesis. *Nat Genet.* 2009 Dec;41(12):1295–302. PMCID: PMC2787691
27. Zhang Y, Yokoyama S, Herriges JC, Zhang Z, Young RE, Verheyden JM, et al. E3 ubiquitin ligase RFWD2 controls lung branching through protein-level regulation of ETV transcription factors. *Proceedings of the National Academy of Sciences. National Acad Sciences;* 2016 Jun 22;:201603310. PMCID: PMC4941481
28. Herriges JC, Verheyden JM, Zhang Z, Sui P, Zhang Y, Anderson MJ, et al. FGF-Regulated ETV Transcription Factors Control FGF-SHH Feedback Loop in Lung Branching. *Developmental Cell.* 2015 Nov;35(3):322–32. PMCID: PMC4763945
29. Abler LL, Mansour SL, Sun X. Conditional gene inactivation reveals roles for Fgf10 and Fgfr2 in establishing a normal pattern of epithelial branching in the mouse lung. *Dev. Dyn.* 2009 Aug;238(8):1999–2013. PMCID: PMC3538083
30. Harris-Johnson KS, Domyan ET, Vezina CM, Sun X. beta-Catenin promotes respiratory progenitor identity in mouse foregut. *Proceedings of the National Academy of Sciences.* 2009 Sep 22;106(38):16287–92. PMCID: PMC2740732
31. Sekine K, Ohuchi H, Fujiwara M, Yamasaki M, Yoshizawa T, Sato T, et al. Fgf10 is essential for limb and lung formation. *Nat Genet.* 1999 Jan;21(1):138–41.
32. Desai TJ, Malpel S, Flentke GR, Smith SM, Cardoso WV. Retinoic acid

selectively regulates Fgf10 expression and maintains cell identity in the prospective lung field of the developing foregut. *Developmental Biology*. 2004 Sep 15;273(2):402–15.

33. Desai TJ, Chen F, Lü J, Qian J, Niederreither K, Dollé P, et al. Distinct roles for retinoic acid receptors alpha and beta in early lung morphogenesis. *Developmental Biology*. 2006 Mar 1;291(1):12–24.
34. Zhao R, Fallon TR, Saladi SV, Pardo-Saganta A, Villoria J, Mou H, et al. Yap tunes airway epithelial size and architecture by regulating the identity, maintenance, and self-renewal of stem cells. *Developmental Cell*. 2014 Jul 28;30(2):151–65. PMID: PMC4130488
35. Lange AW, Sridharan A, Xu Y, Stripp BR, Perl A-K, Whitsett JA. Hippo/Yap signaling controls epithelial progenitor cell proliferation and differentiation in the embryonic and adult lung. *Journal of Molecular Cell Biology*. Oxford University Press; 2015 Feb;7(1):35–47. PMID: PMC4400400
36. Mahoney JE, Mori M, Szymaniak AD, Varelas X, Cardoso WV. The Hippo Pathway Effector Yap Controls Patterning and Differentiation of Airway Epithelial Progenitors. *Dev. Cell*. Elsevier Inc; 2014 Jul 16;:1–14.
37. Ornitz DM, Yin Y. Signaling Networks Regulating Development of the Lower Respiratory Tract. *Cold Spring Harb Perspect Biol*. Cold Spring Harbor Lab; 2012 May 1;4(5):a008318–8. PMID: PMC3331697
38. Longmire TA, Ikonomou L, Hawkins F, Christodoulou C, Cao Y, Jean JC, et al. Efficient derivation of purified lung and thyroid progenitors from embryonic stem cells. *Cell Stem Cell*. 2012 Apr 6;10(4):398–411. PMID: PMC3322392
39. Huang SXL, Islam MN, O'Neill J, Hu Z, Yang Y-G, Chen Y-W, et al. efficient generation of lung and airway epithelial cells from human pluripotent stem cells. *Nat Biotechnol*. Nature Publishing Group; 2013 Dec 1;:1–11. PMID: PMC4101921
40. Firth AL, Dargitz CT, Qualls SJ, Menon T, Wright R, Singer O, et al. Generation of multiciliated cells in functional airway epithelia from human induced pluripotent stem cells. *Proceedings of the National Academy of Sciences*. 2014 Apr 29;111(17):E1723–30. PMID: PMC4035971
41. Konishi S, Gotoh S, Tateishi K, Yamamoto Y, Korogi Y, Nagasaki T, et al. Directed Induction of Functional Multi-ciliated Cells in Proximal Airway Epithelial Spheroids from Human Pluripotent Stem Cells. *Stem Cell Reports*. Elsevier; 2015 Dec;0(0).
42. Gotoh S, Ito I, Nagasaki T, Yamamoto Y, Konishi S, Korogi Y, et al. Generation of alveolar epithelial spheroids via isolated progenitor cells from

human pluripotent stem cells. *Stem Cell Reports*. Elsevier; 2014 Sep 9;3(3):394–403. PMID: PMC4266003

43. Ghaedi M, Calle EA, Mendez JJ, Gard AL, Balestrini J, Booth A, et al. Human iPS cell-derived alveolar epithelium repopulates lung extracellular matrix. *J. Clin. Invest.* 2013 Nov 1;123(11):4950–62. PMID: PMC3809786
44. Gilpin SE, Ren X, Okamoto T, Guyette JP, Mou H, Rajagopal J, et al. Enhanced lung epithelial specification of human induced pluripotent stem cells on decellularized lung matrix. *Ann. Thorac. Surg.* 2014 Nov;98(5):1721–9–discussion1729. PMID: PMC4252658
45. Hashimoto S, Chen H, Que J, Brockway BL, Drake JA, Snyder JC, et al. β -Catenin-SOX2 signaling regulates the fate of developing airway epithelium. *Journal of Cell Science*. 2012 Feb 15;125(Pt 4):932–42. PMID: PMC3311930
46. Que J, Okubo T, Goldenring JR, Nam KT, Kurotani R, Morrissey EE, et al. Multiple dose-dependent roles for Sox2 in the patterning and differentiation of anterior foregut endoderm. *Development*. 2007 May 23;134(13):2521–31.
47. Chang DR, Martinez Alanis D, Miller RK, Ji H, Akiyama H, McCrea PD, et al. Lung epithelial branching program antagonizes alveolar differentiation. *Proceedings of the National Academy of Sciences*. 2013 Sep 20. PMID: PMC3831485
48. Moens CB, Auerbach AB, Conlon RA, Joyner AL, Rossant J. A targeted mutation reveals a role for N-myc in branching morphogenesis in the embryonic mouse lung. *Genes Dev. Cold Spring Harbor Lab*; 1992 May 1;6(5):691–704.
49. Okubo T, Knoepfler PS, Eisenman RN, Hogan BLM. Nmyc plays an essential role during lung development as a dosage-sensitive regulator of progenitor cell proliferation and differentiation. *Development*. The Company of Biologists Ltd; 2005 Mar 15;132(6):1363–74.
50. Perl A-KT, Kist R, Shan Z, Scherer G, Whitsett JA. Normal lung development and function after Sox9 inactivation in the respiratory epithelium. *genesis*. 2005 Jan;41(1):23–32.
51. Rockich BE, Hrycaj SM, Shih H-P, Nagy MS, Ferguson MAH, Kopp JL, et al. Sox9 plays multiple roles in the lung epithelium during branching morphogenesis. *Proceedings of the National Academy of Sciences*. 2013 Nov 4. PMID: PMC3839746
52. Cardoso WV, Itoh A, Nogawa H, Mason I, Brody JS. FGF-1 and FGF-7 induce distinct patterns of growth and differentiation in embryonic lung

epithelium. *Dev. Dyn.* Wiley-Liss, Inc; 1997 Mar;208(3):398–405.

53. Min H, Danilenko DM, Scully SA, Bolon B, Ring BD, Tarpley JE, et al. Fgf-10 is required for both limb and lung development and exhibits striking functional similarity to *Drosophila* branchless. *Genes & Development*. 1998 Oct 15;12(20):3156–61. PMID: PMC317210
54. Nyeng P, Norgaard GA, Kobberup S, Jensen J. FGF10 maintains distal lung bud epithelium and excessive signaling leads to progenitor state arrest, distalization, and goblet cell metaplasia. *BMC Dev Biol*. 2008;8(1):2.
55. Volckaert T, Campbell A, Dill E, Li C, Minoo P, De Langhe S. Localized Fgf10 expression is not required for lung branching morphogenesis but prevents differentiation of epithelial progenitors. *Development*. The Company of Biologists Limited; 2013 Sep;140(18):3731–42. PMID: PMC3754473
56. Kadzik RS, Cohen ED, Morley MP, Stewart KM, Lu MM, Morrissey EE. Wnt ligand/Frizzled 2 receptor signaling regulates tube shape and branch-point formation in the lung through control of epithelial cell shape. *Proceedings of the National Academy of Sciences*. 2014 Aug 26;111(34):12444–9. PMID: PMC4151720
57. Mucenski ML, Nation JM, Thitoff AR, Besnard V, Xu Y, Wert SE, et al. β -Catenin regulates differentiation of respiratory epithelial cells in vivo. 2005.
58. Mucenski ML, Wert SE, Nation JM, Loudy DE, Huelsken J, Birchmeier W, et al. beta-Catenin is required for specification of proximal/distal cell fate during lung morphogenesis. *J. Biol. Chem*. 2003 Oct 10;278(41):40231–8.
59. Elluru RG, Whitsett JA. Potential role of Sox9 in patterning tracheal cartilage ring formation in an embryonic mouse model. *Arch. Otolaryngol. Head Neck Surg*. 2004 Jun;130(6):732–6. PMID: PMC2636717
60. Weaver M, Yingling JM, Dunn NR, Bellusci S, Hogan BL. Bmp signaling regulates proximal-distal differentiation of endoderm in mouse lung development. *Development*. 1999 Sep;126(18):4005–15.
61. Malpel S, Mendelsohn C, Cardoso WV. Regulation of retinoic acid signaling during lung morphogenesis. *Development*. 2000 Jul;127(14):3057–67.
62. Chen F, Cao Y, Qian J, Shao F, Niederreither K, Cardoso WV. A retinoic acid-dependent network in the foregut controls formation of the mouse lung primordium. *J. Clin. Invest*. 2010 Jun;120(6):2040–8. PMID: PMC2877937
63. Wong AP, Bear CE, Chin S, Pasceri P, Thompson TO, Huan L-J, et al.

Directed differentiation of human pluripotent stem cells into mature airway epithelia expressing functional CFTR protein. *Nat Biotechnol.* 2012 Aug 26.

64. Gilpin SE, Ren X, Okamoto T, Guyette JP, Mou H, Rajagopal J, et al. Enhanced Lung Epithelial Specification of Human Induced Pluripotent Stem Cells on Decellularized Lung Matrix. *Ann. Thorac. Surg.* 2014 Nov;98(5):1721–9.
65. Mou H, Zhao R, Sherwood R, Ahfeldt T, Lapey A, Wain J, et al. Generation of Multipotent Lung and Airway Progenitors from Mouse ESCs and Patient-Specific Cystic Fibrosis iPSCs. *Cell Stem Cell.* 2012 Apr 6;10(4):385–97. PMID: PMC3474327
66. Ornitz DM, Xu J, Colvin JS, McEwen DG, MacArthur CA, Coulier F, et al. Receptor specificity of the fibroblast growth factor family. *J. Biol. Chem. American Society for Biochemistry and Molecular Biology*; 1996 Jun 21;271(25):15292–7.
67. Zhang X, Ibrahimi OA, Olsen SK, Umemori H, Mohammadi M, Ornitz DM. Receptor specificity of the fibroblast growth factor family. The complete mammalian FGF family. *J. Biol. Chem. American Society for Biochemistry and Molecular Biology*; 2006 Jun 9;281(23):15694–700. PMID: PMC2080618
68. Tichelaar JW, Lu W, Whitsett JA. Conditional expression of fibroblast growth factor-7 in the developing and mature lung. *Journal of Biological Chemistry.* 2000.
69. Makarenkova HP, Hoffman MP, Beenken A, Eliseenkova AV, Meech R, Tsau C, et al. Differential interactions of FGFs with heparan sulfate control gradient formation and branching morphogenesis. *Sci Signal.* 2009 Sep 15;2(88):ra55–5. PMID: PMC2884999
70. Lee J-H, Bhang DH, Beede A, Huang TL, Stripp BR, Bloch KD, et al. Lung Stem Cell Differentiation in Mice Directed by Endothelial Cells via a BMP4-NFATc1-Thrombospondin-1 Axis. *Cell.* 2014 Jan 30;156(3):440–55. PMID: PMC3951122
71. Kaarteenaho R, Lappi-Blanco E, Lehtonen S. Epithelial N-cadherin and nuclear β -catenin are up-regulated during early development of human lung. *BMC Dev Biol. BioMed Central*; 2010 Nov 16;10(1):113.
72. Dye BR, Miller AJ, Spence JR. How to Grow a Lung: Applying Principles of Developmental Biology to Generate Lung Lineages from Human Pluripotent Stem Cells. *Curr Pathobiol Rep. Springer US*; 2016 Apr 18;:1–11.
73. D'Amour KA, Agulnick AD, Eliazer S, Kelly OG, Kroon E, Baetge EE.

Efficient differentiation of human embryonic stem cells to definitive endoderm. *Nat Biotechnol* [Internet]. 2005 Oct 28;23(12):1534–41. Retrieved from: <http://www.nature.com/nbt/journal/v23/n12/abs/nbt1163.html>

74. Spence JR, Mayhew CN, Rankin SA, Kuhar MF, Vallance JE, Tolle K, et al. Directed differentiation of human pluripotent stem cells into intestinal tissue in vitro. *Nature*. 2011 Feb 3;470(7332):105–9. PMID: PMC3033971
75. Green MD, Chen A, Nostro M-C, d'Souza SL, Schaniel C, Lemischka IR, et al. Generation of anterior foregut endoderm from human embryonic and induced pluripotent stem cells. *Nat Biotechnol*. Nature Publishing Group; 2011 Feb 27;:1–7.
76. Zhang M, Wang H, Teng H, Shi J, Zhang Y. Expression of SHH signaling pathway components in the developing human lung. *Histochem. Cell Biol*. 2010 Oct;134(4):327–35.
77. Kopp JL, Dubois CL, Schaffer AE, Hao E, Shih HP, Seymour PA, et al. Sox9+ ductal cells are multipotent progenitors throughout development but do not produce new endocrine cells in the normal or injured adult pancreas. *Development*. 2011 Jan 25;138(4):653–65. PMID: PMC3026412
78. del Moral P-M, Warburton D. Explant culture of mouse embryonic whole lung, isolated epithelium, or mesenchyme under chemically defined conditions as a system to evaluate the molecular mechanism of branching morphogenesis and cellular differentiation. *Methods Mol. Biol*. 2010;633:71–9. PMID: PMC3120103
79. Bagai S, Rubio E, Cheng J-F, Sweet R, Thomas R, Fuchs E, et al. Fibroblast growth factor-10 is a mitogen for urothelial cells. *J. Biol. Chem*. 2002 Jun 28;277(26):23828–37.
80. Spence JR, Lange AW, Lin S-CJ, Kaestner KH, Lowy AM, Kim I, et al. Sox17 Regulates Organ Lineage Segregation of Ventral Foregut Progenitor Cells. *Developmental Cell*. Elsevier Ltd; 2009 Jul 21;17(1):62–74. PMID: PMC2734336
81. Kim CFB, Jackson EL, Woolfenden AE, Lawrence S, Babar I, Vogel S, et al. Identification of bronchioalveolar stem cells in normal lung and lung cancer. *Cell*. 2005 Jun 17;121(6):823–35.

Figure legends:

Figure 1. FGF7 supports growth and is permissive for differentiation of mouse embryonic lung distal-tip progenitors.

(A) Schematic of Sox9-eGFP distal lung buds dissected at E13.5 and cultured in a Matrigel droplet.

(B) Low magnification images of isolated lung buds under brightfield (left) or showing Sox9-eGFP expression (right). Scale bar represents 200um.

(C) Buds were cultured in basal media or individually with different factors (10ng/mL FGF7, 10ng/mL FGF10, 10ng/mL BMP4, 50nM RA, 3uM CHIR-99021) and imaged at Day 0, Day 5 and Day 14 in culture. Scale bar represents 200um.

(D) All 5 factors ('5F'; FGF7, FGF10, BMP4, RA, CHIR-99021) were combined, or, FGF7 was removed (5F-FGF7) and growth was monitored for 5 days (left two panels). Bud growth was compared for 5 days side-by-side in a low-dose of FGF7 (10ng/mL) and in a high dose of FGF10 (500ng/mL) (right two panels). Scale bar represents 200um.

(E-F) FGF7 cultured tissue was interrogated for differentiation after 2 weeks *in vitro* (E) and was compared to the developing mouse lung *in vivo* (F). Low magnification images (top row in E, F) or at high magnification (bottom row in E, F). Differentiation markers examined include AQP5 (AECI), SFTPB (AECII), SCGB1A1 (club cell), Acetylated-TUBULIN (Ac-Tub; multiciliated cells), P63 (Basal cells). Scale bars in the top and bottom rows represent 50um.

(G) QRT-PCR across time in culture with FGF7 indicated that the tissue began to increase expression levels of differentiated cell markers *Scgb1a1*, *Sftpb* and *Aqp5*, and showed a decrease in the expression of the progenitor marker, *Sox9*. Each data point represents the mean (+/- SEM) of 3 independent biological replicates (n=3).

Figure 1, Supplement 1. FGF7 induces proliferation in a dose-dependent manner in *ex vivo* cultured murine lung buds.

(A) Isolated E13.5 embryonic mouse lung buds from wild type versus Sox9-eGFP mice did not have significantly different levels of Sox9 transcript as shown by qPCR. Each data point represents an independent biological replicate.

(B) Lung buds were grown in increasing concentrations of FGF7 and examined after 3 days and 5 days *in vitro*. 0ng/mL (basal media) did not induce bud growth, whereas 1ng/mL induced very modest growth, and all other conditions supported robust growth for 5 days *in vitro*. Scale bar represents 200um.

(C) Cultured buds were pulse labeled for 1 hour with EdU and the percent of total cell labeled was quantified by Flow Cytometry. Low doses of FGF7 (1-10ng/mL) had a similar proportion of cells labeled whereas treatment with 50-100 ng/mL resulted in a significant increase in labeled cells. Each data point represents an independent biological replicate.

(D) Lung bud explants grown in FGF7 for two weeks did not contain cells that were double positive for SCGB1A1 and SFTPC indicating that the explants did not possess bronchoalveolar stem cells(81). Scale bar represents 50um.

(E) Sox9-Cre^{ER};Rosa26^{Tomato} lungs were induced with Tamoxifen 24 hours prior to isolation of the buds, which were isolated and cultured at E13.5. Lineage labeled buds demonstrated that labeled cells expanded in culture over the course of two weeks. Asterisks (*) mark air bubbles within Matrigel droplets that were auto-fluorescent, and arrowheads point to day 0 isolated lung buds. Scale bar represents 200um.

Figure 2. Synergistic activity of FGF7, CHIR-99021 and RA maintain tip-progenitor-like cells in mouse lung bud explants.

(A-B) Buds were explanted and grown with 5F media minus one growth factor to identify conditions that allowed buds to expand (A) and maximized of expression of Sox9 mRNA (B). Removing BMP4 from the 5F media (5F-BMP4) led to a significant increase in Sox9 expression after 5 days when compared to the full 5F media and resulted in expression levels closest to those of freshly isolated E13.5 lung buds. All groups exhibited low levels of Sox2 expression. Each data point in (B) represents an independent biological replicate. Scale bar represents 200um.

(C-D) After removing BMP4, the minimum combination of factors that interact with FGF7 to promote growth (C) and maintain high expression of distal progenitor markers was assessed. Treatment with '4F' media (FGF7/FGF10/CHIR-99021/RA) or '3F' media (FGF7/CHIR-99021/RA) led to growth and had the highest levels of Sox9 expression when compared to FGF7 alone. All groups exhibited maintenance of the progenitor markers *Id2* and *N-myc* and had low levels of proximal marker Sox2. Each data point in (D) represents an independent biological replicate. Scale bar represents 500um.

(E-F) Section and whole mount immunohistochemical staining analysis confirmed that 3F and 4F conditions maintained robust SOX9 protein staining.

Figure 2, Supplement 1. Synergistic activity of FGF7, CHIR-99021 and RA expands Sox9-lineage labeled murine distal epithelial lung progenitors.

(A-B) E13.5 mouse lung buds were explanted and grown with 5F media, and 5F minus one growth factor. Gene expression was examined in each condition after 2 weeks in culture for differentiation markers of alveolar cell types (A) and airway cell types (B), including *Aqp5* (AECI), *Sftpb* (AECII), *p63* (basal cell), *Foxj1* (multiciliated cells), *Scgb1a1* (club cells). Each data point represents an independent biological replicate.

(C-D) E13.5 mouse lung buds were explanted and grown with different combinations of growth factors, including '4F' media (FGF7/FGF10/CHIR-99021/RA) or '3F' media (FGF7/CHIR-99021/RA), in addition to FGF7/CHIR-99021 and FGF7/RA. Gene expression for proximal airway markers (C) and maintained levels of mature proximal (C) and distal alveolar (D) markers were assessed after 2 weeks in culture. Each data point represents an independent biological replicate.

(E) Sox9-Cre^{ER};Rosa26^{Tomato} lungs were induced with Tamoxifen 24 hours prior to isolation of the buds, which were isolated and cultured at E13.5. Lineage labeled buds demonstrated that labeled cells expanded in culture over the course of two weeks in all conditions tested. Scale bar represents 200um.

(F) To identify whether cultured lung buds were able to undergo phenotypic maturation, buds were grown for 5 days in 4F media and then either maintained for an additional 4 days in 4F media or switched to FGF7 alone. Scale bar represents 200um.

(G) After 9 days in culture (as shown in (F)), protein staining for SOX9, SFTPC and AQP5 was carried out (top row), and staining was compared to *in vivo* developing lungs at E16.5 and P0 (bottom row). Buds grown for 9 days in 4F media possessed many cells that co-expressed SOX9/SFTPC or SOX9/AQP5 whereas those grown in FGF7 media alone contain cells that are positive for AQP5 or SFTPC, but do not express SOX9. Phenotypically, *in vitro* grown buds that are exposed to FGF7 alone are similar to AQP5+ AECI and SFTPC+ AECII cells in the P0 mouse lung *in vivo*. Scale bar represents 50um

(H-J) QRT-PCR analysis after 9 days in culture (as shown in (F)) confirms that Sox9 expression is reduced in buds that are switched to FGF7 media compared to 4F media (H), while the club cell marker *Scgb1a1* was increased (J) in buds switched to FGF7 media. Significant changes in other markers were not observed (I-J). Each data point in (H-J) represents an independent biological replicate.

Figure 3. Synergistic activity of FGF7, CHIR-99021 and RA expands and maintains distal tip-progenitor cells in human fetal lung buds cultured *ex vivo*.

(A-B) Distal epithelial lung bud tips were collected from ~12 week old human fetal lungs and cultured in Matrigel. Scalebar in (B) represents 500um.

(C) Freshly isolated buds were immunostained for SOX9, SOX2, ECAD and DAPI and wholmount imaged. Z-stacks were 3D rendered, and resulting images demonstrated overlapping SOX2 and SOX9 expression at bud tips. Scalebar represents 100um.

(D) Overlapping SOX9/SOX2 protein expression at distal bud tips was confirmed in formalin fixed, paraffin embedded sections from a 14 week old human fetal lung specimen.

(E) Isolated human fetal lung buds were cultured for over 6 weeks various media combinations (optimized in mouse lung bud cultures as shown in Figures 1 and 2) to determine conditions that supported tissue growth/expansion. FGF7 alone

supported an initial expansion of buds, but the tissue stopped expanding beyond the 4 week period. All other combinations appeared to support robust lung bud expansion up to 6 weeks in culture. Scale bar represents 500um.

(F-G) Immunostaining in sections (F) or in wholemount (G) demonstrated that lung buds expanded in 3F or 4F media after 4 weeks *in vitro* maintained robust co-expression of SOX9 and SOX2. FGF7 grown buds expressed both markers, but strong cytoplasmic SOX9 localization was observed. FGF7/CHIR-99021 and FGF7/RA conditions showed weak staining. Scalebar in (F) represents 50um, and in (G) represents 100um.

(H) QRT-PCR analysis after 4 weeks *in vitro* showed that 3F and 4F conditions maintained the highest levels of SOX9, which were not significantly different from levels seen in the human fetal lung (H), while also maintaining robust expression of distal progenitor markers SOX2, *NMYC* and *ID2* when compared to FGF7 alone, FGF7/CHIR-99021 or FGF7/RA. Each data point represents an independent biological replicate.

Figure 3, Supplement 1. Characterizing human fetal lung buds *in situ* and in culture.

(A) Human fetal epithelial buds expanded in different media combinations were assessed for differentiation markers using QRT-PCR after 4 weeks in culture. FGF7-only media led to significantly increased expression of the proximal airway markers *P63* and *SCGB1A1* compared to the 14 week old human fetal lung ('Fetal'), whereas treatment with 3F or 4F media kept the expression levels of mature proximal markers *P63*, *FOXJ1* and *SCGB1A1* at or below the levels seen in human fetal lung. Each data point represents an independent biological replicate.

(B) Treatment with 3F or 4F media significantly increased the expression of the AECII marker *SFTPB* compared to human fetal lung expression and FGF7-only, but did not lead to increased expression of the AECI marker *HOPX*.

(C) Paraffin embedded sections from human fetal lung specimens from 10-20 weeks demonstrate that distal epithelial progenitor regions are SOX9/SOX2 double-positive until 14 weeks, but lose this property sometime between 14 and 16 weeks gestation. By 16 weeks distal buds are SOX9+/SOX2- and a clear transition zone is established where cells are negative for both SOX2 and SOX9. Scale bar represents XXum.

(D) High concentrations of FGF10 do not lead to expansion of human fetal lung buds. Isolated tip-progenitors were cultured with in basal media or 500 ng/mL of FGF10. Bud tips were observed to form small cysts in FGF10 at this concentration; however, expansion of the tissue was not robust. Similarly, bud tips treated with the Rho-kinase (Rock) inhibitor Y27632 did not lead to tissue expansion; however, treatment with FGF10 (500ng/mL) plus Y27632 led to robust cyst formation and tissue expansion. This indicated that the effect of high concentrations of FGF10 alone had limited effects on isolated human fetal buds. Dashed lines highlight the Matrigel droplet.

Figure 4. Synergistic activity of FGF7, CHIR-99021 and RA induces and maintains a population of distal lung tip-progenitor-like cells in hPSCs.

(A-B) Foregut spheroids were cultured with 3F media (FGF7, CHIR-99021 and RA) and brightfield images were collected over time *in vitro*. Spheroids exhibited stereotyped growth over time and resulted in highly complex epithelial structures, called Human Lung Organoid, grown in 3F media (3F HLOs). Scale bars represent 200um. Note: In panel (B) the same spheroid is imaged for Day 1 through Day 9; however, representative images of different organoids are shown on Day 14 and Day 45.

(C) 3F HLOs exhibited robust NKX2.1 protein expression by immunofluorescence after 40 days *in vitro*, demonstrating a lung lineage. Scale bar represents 100um.

(D) 3F HLOs exhibited apparent proximal-distal patterning after 40 days *in vitro*, where immunofluorescence demonstrated that budded domains at the periphery of the 3D structure co-expressed SOX9/SOX2, consistent with the human fetal lung, and interior regions of the structures contained SOX2+ cells that were negative for SOX9. Scale bar represents 100um.

(E) Immunofluorescence showed that SOX9/SOX2 double positive peripheral regions were maintained for up to 115 days in 3F media. Cellular debris can be seen within the lumen of the HLOs. Scale bar represents 100um.

(F) After 4 weeks in culture, 3F HLOs were compared to distal regions of the human fetal lung (epithelium plus mesenchyme) using QRT-PCR. 3F HLOs exhibited significantly lower levels of SOX9 transcript, but similar levels of other transcripts found in the human fetal lung, including *NMYC*, *ID2* and *SOX2*. Each data point represents an independent biological replicate.

(G) A QRT-PCR comparison was also performed between hPSCs, foregut (FG) spheroids, isolated human fetal buds and isolated peripheral budded regions from 3F HLOs (after 6 weeks *in vitro*). In this analysis, 3F HLOs and human fetal buds expressed similar levels of SOX9, SOX2, *NMYC* and *ID2*. Each data point represents an independent biological replicate. Different shapes indicate biological replicates in the human fetal bud sample, and each point for the same shape represents a technical replicates.

(H-J) Interior regions of 3F HLOs (top row) possessed cells expressing markers of secretory cells, including SCGB1A1 (club cells) (H) and MUC5AC (goblet cells) (I) when compared to adult human airway tissue (bottom row). Notably, 3F HLOs lacked P63+ cells (H) and demonstrated AC-TUB staining, which was not localized to *bona fide* multiciliated structures (H). 3F HLOs also demonstrated evidence of goblet cells (arrowheads) and mucous secretion within the lumen as shown by PAS Alcian Blue staining (J). Scalebars in (H) represent 50um and apply to low and high magnification images in (H) and (I), respectively. Scale bars in (J) represent 100um.

Figure 4, Supplement 1. In vitro expansion, growth and passaging of 3F HLOs.

(A-B) Generation of 3F HLOs is robust. A single 24 well plate of hPSC cultures yield hundreds of foregut spheroids, which are expanded in Matrigel droplets in a new 24 well plate (A, B). Many foregut spheroids are placed into each droplet of Matrigel and expanded (A), and cultures grow substantially after 7 days (A) and are subsequently split into new Matrigel droplets every two weeks to provide room for growth and expansion (B). 3F HLOs are visible to the eye without a microscope by day 35 (B). Scale bar in (A) represents 1mm.

(C-D) 3F HLOs undergo stereotyped growth, starting with epithelial expansion and folding from day ~20 through day ~35, followed by the emergence of bud-like domains and apparent bifurcation of bud tips (D). Asterisks indicate bud-like domains that appear to bifurcate over time. Scale bars in (C, D) represent 200um.

(E-G) 3F HLOs can be serially split and expanded by mechanical shearing through a 27-gauge needle. Following passaging, 3F HLOs maintain a cystic structure (E), which allows for rapid expansion of the population (F). The majority HLOs resulting from needle passaging are double positive for SOX9 and SOX2 (G), suggesting a selection for the distal progenitor-like population. Scale bar in (E) represents 1mm, and in (G) represents 50um.

Figure 4, Supplement 2. Characterizing 'epithelial' and 'dense' phenotypes in HLOs.

(A-B) HLOs exhibited 2 major phenotypes when grown in 3F media, termed 'epithelial' (as characterized in Figures 3-5) and 'dense'. We also observed many HLOs that were a mix of these 2 phenotypes, termed 'mixed' (A). When grown in FGF7 alone, 90% of HLOs exhibited a 'dense' phenotype with no clear epithelial structures, whereas 5% of the FGF7 HLOs contained a clear epithelial phenotype (A, B). 3F and 4F media contained HLOs that were either entirely epithelial in nature, entirely 'dense', or mixed, in various proportions (A-B). Scale bar in (A) represents 200um.

(C-D) After 42 days *in vitro*, dense 3F HLOs were assessed by immunofluorescence. Dense 3F HLOs consisted predominantly of cells expressing the markers HOPX (C) and PDPN (D), which is consistent with AECI cells in the adult alveoli (C, bottom row). Notably, dense 3F HLOs did not express SFTP (C), but maintained expression of SOX9 (D). Scale bar represents 50um.

(E-G) After 42 days *in vitro*, dense 3F HLOs were compared to epithelial 3F HLOs and whole fetal lung tissue by QRT-PCR. Consistent with immunostaining data, dense 3F HLOs were enriched for *HOPX* mRNA compared to epithelial HLOs or human fetal lung tissue (H). In general, both dense and epithelial 3F HLOs had lower expression of differentiated cell markers, and in the general lung epithelial marker, *NKX2.1* was reduced compared to the fetal lung, consistent with our previously published lung organoid data(2). Each data point represents an independent biological replicate.

Figure 5. 3F Media is required for prolonged maintenance of distal progenitor-like cells in HLOs.

(A) Schematic of the experimental setup in Figure 5. HLOs were generated and grown in 3F media for 42 days, at which time, half of the tissue was maintained in 3F for an additional 26 days while the other half was switched to FGF7-only media.

(B) Wholmount brightfield imaging revealed that HLOs grown in 3F maintained bud-like structures for the duration of the experiment (top), whereas FGF7-only HLOs lost bud-like structures and the epithelium appeared smooth on the outer surface of the 3D structure (bottom). Scalebar represents 500um.

(C) Peripheral budded regions of 3F HLOs showed nuclear SOX9/SOX2 co-staining (top row), whereas FGF7-only HLOs exhibited a loss of double-positive cells (middle and bottom row). FGF7-only HLOs still expressed SOX2 and SOX9, but we observed that SOX9 expression appeared cytoplasmic (middle row), and was not co-expressed in the same domains as SOX2 (bottom row). Scale bar represents 50um.

(D) QRT-PCR analysis comparing 3F HLOs and FGF7-only HLOs demonstrated that SOX9 expression was not different between groups, whereas SOX2 was increased when grown in FGF7-only. Each data point represents an independent biological replicate.

(E) 3F HLOs and FGF7-only HLOs were examined for expression of the goblet cell marker, MUC5AC. A striking increase in the number of MUC5AC+ cells was observed in FGF7-only, as well as an increase in mucus staining within the lumens of the HLO. Scale bars represent 50um.

(F) *MUC5AC* gene expression levels reflected protein expression in (E), with FGF7-only HLOs having significantly higher mRNA levels compared to 3F HLOs based on QRT-PCR. Each data point represents an independent biological replicate.

(G-H) In 3F HLOs, the basal cell marker, P63, was not observed in immunofluorescent images (G, See also Figure 4H), and *P63* mRNA expression was low based on QRT-PCR (H). In contrast, P63-positive cells were present in FGF7-only HLOs based on immunostaining (G), and *P63* mRNA expression was significantly increased based on QRT-PCR (H). Scale bar in (G) represents 50um. Each data point represents an independent biological replicate.

(I-J) Immunofluorescence (I) and QRT-PCR (J) were used to examine expression of club cell marker SCGB1A1. Cells positive for SCGB1A1 protein staining were observed in both groups (I). While mRNA levels of SCGB1A1 increased 100-fold in HLOs treated with FGF7-only, this increase was not statistically significant (J). Scale bar in (I) represents 50um. Each data point represents an independent biological replicate.

(K-N) Immunofluorescence (K, M) and QRT-PCR (L, N) were used to examine expression of markers for AECII (SFTPC) (K, L) and AECI (PDPN, *HOPX*) (M-N). Protein staining (K) and mRNA (L) for SFTPC showed increased expression in FGF7-only HLOs compared to 3F HLOs, although we also note the high

variability in expression in the 3F HLOs across biological replicates (L). Similarly, Protein staining for PDPN (M) and *HOPX* mRNA (N) showed increased expression in FGF7-only HLOs compared to 3F HLOs. Scale bar in (K, M) represents 50um and applies to all panels in (K) and (M). Each data point in (L) and (N) represents an independent biological replicate.

(O) QRT-PCR analysis showed that mRNA levels of *FOXJ1* were significantly increased in HLOs treated with FGF7-only (O). However, FOXJ1 protein staining was not detected in either group (data not shown). Each data point represents an independent biological replicate.

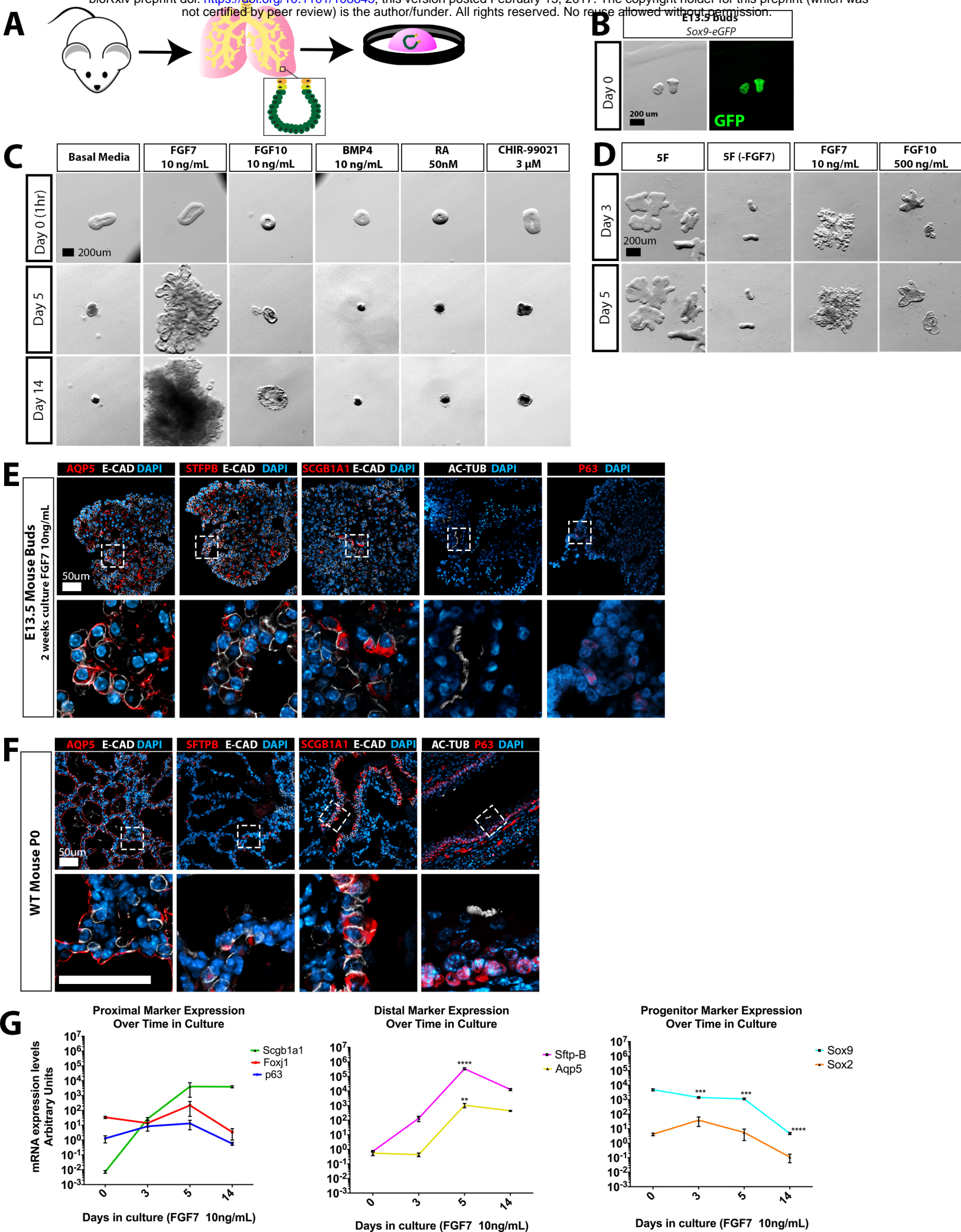


Figure 1, Supplement 1

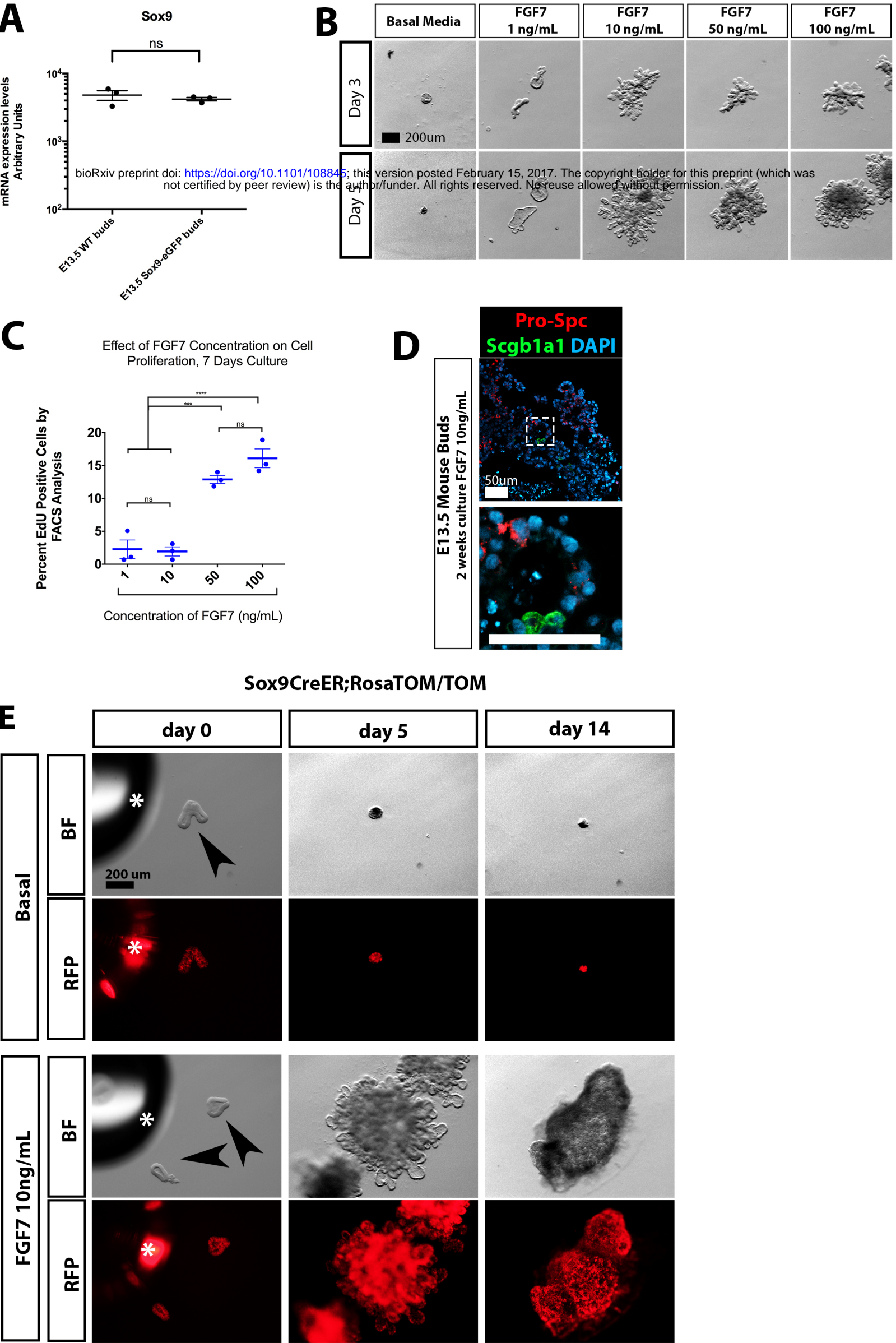
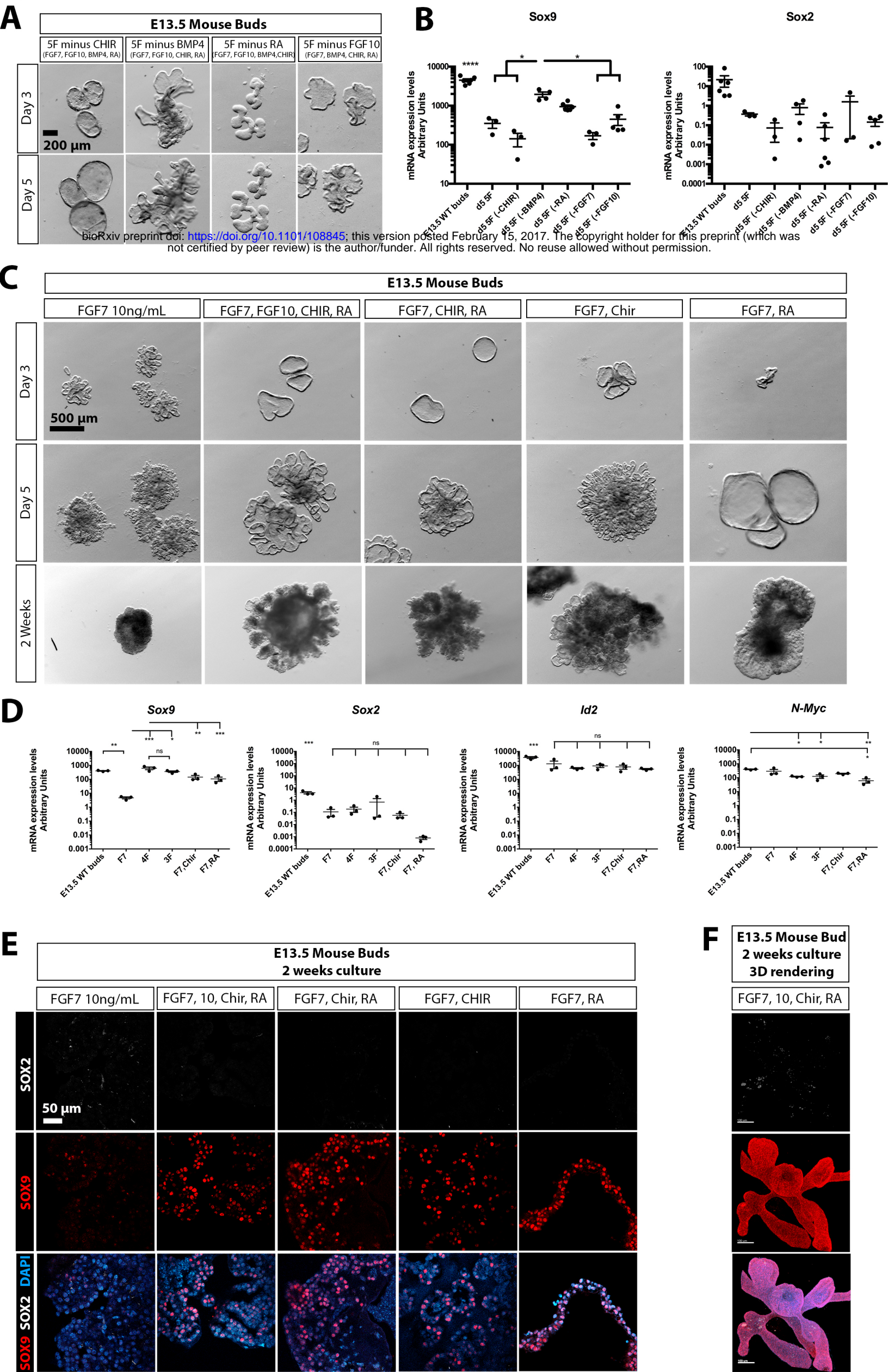


Figure 2



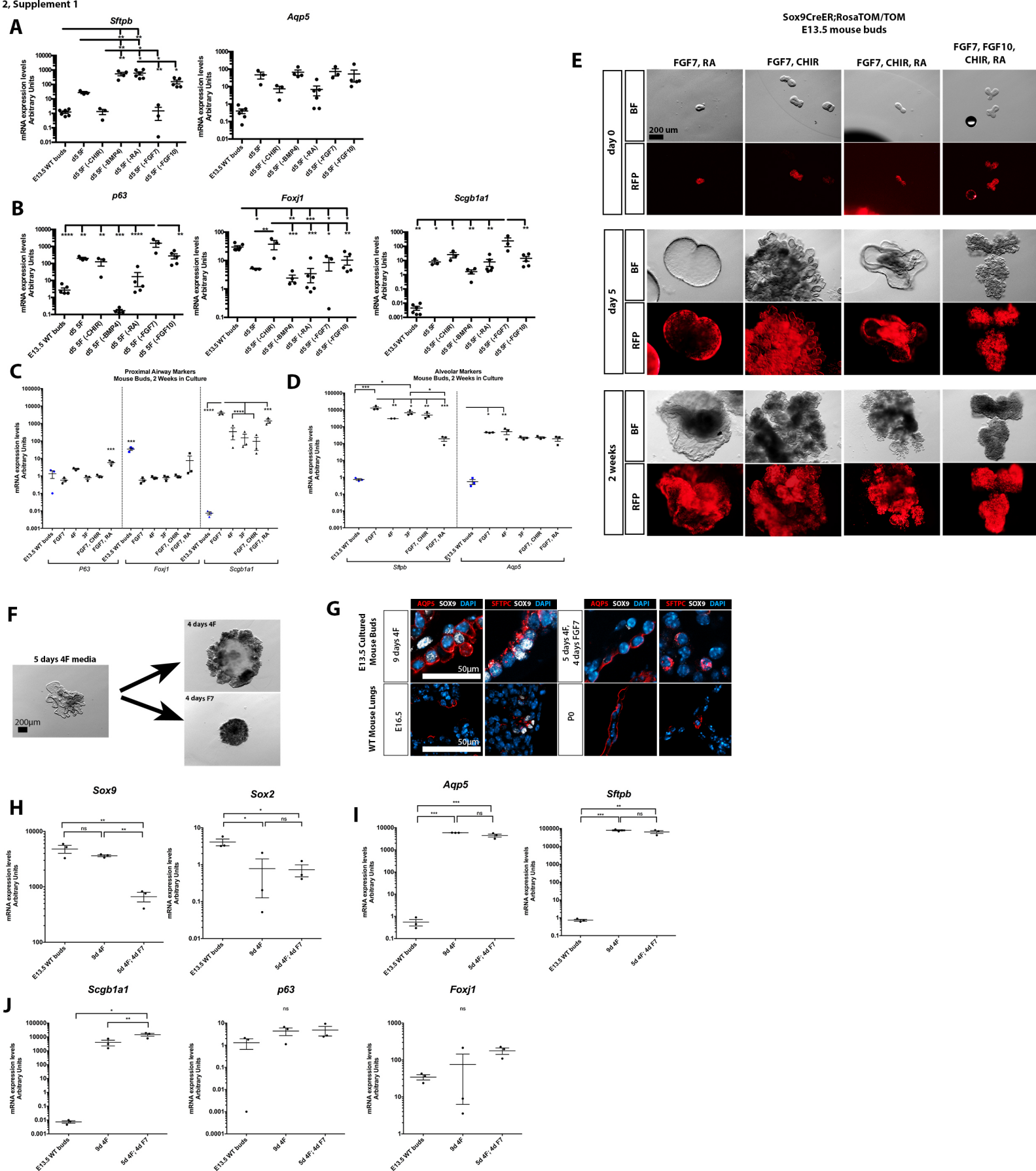
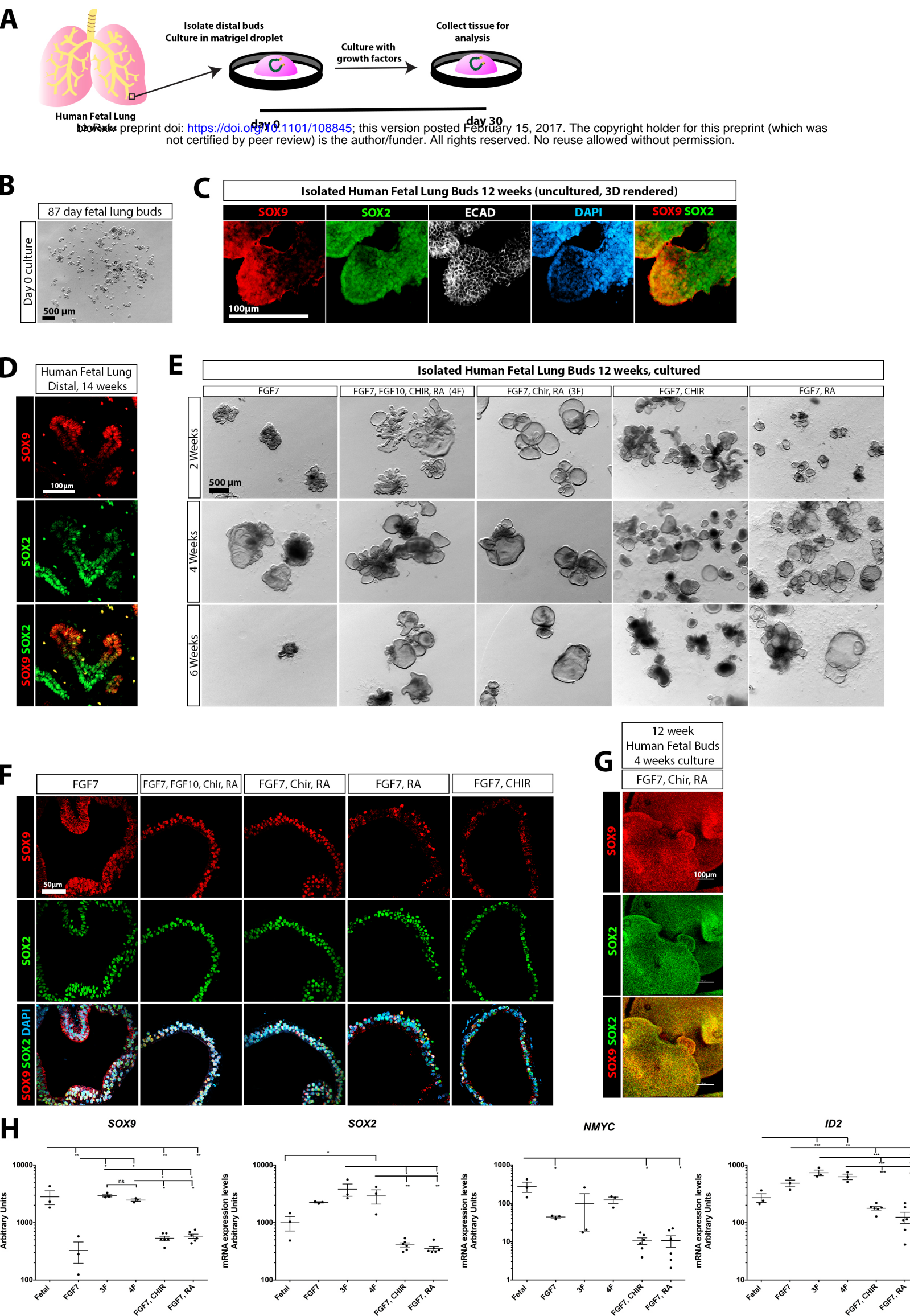
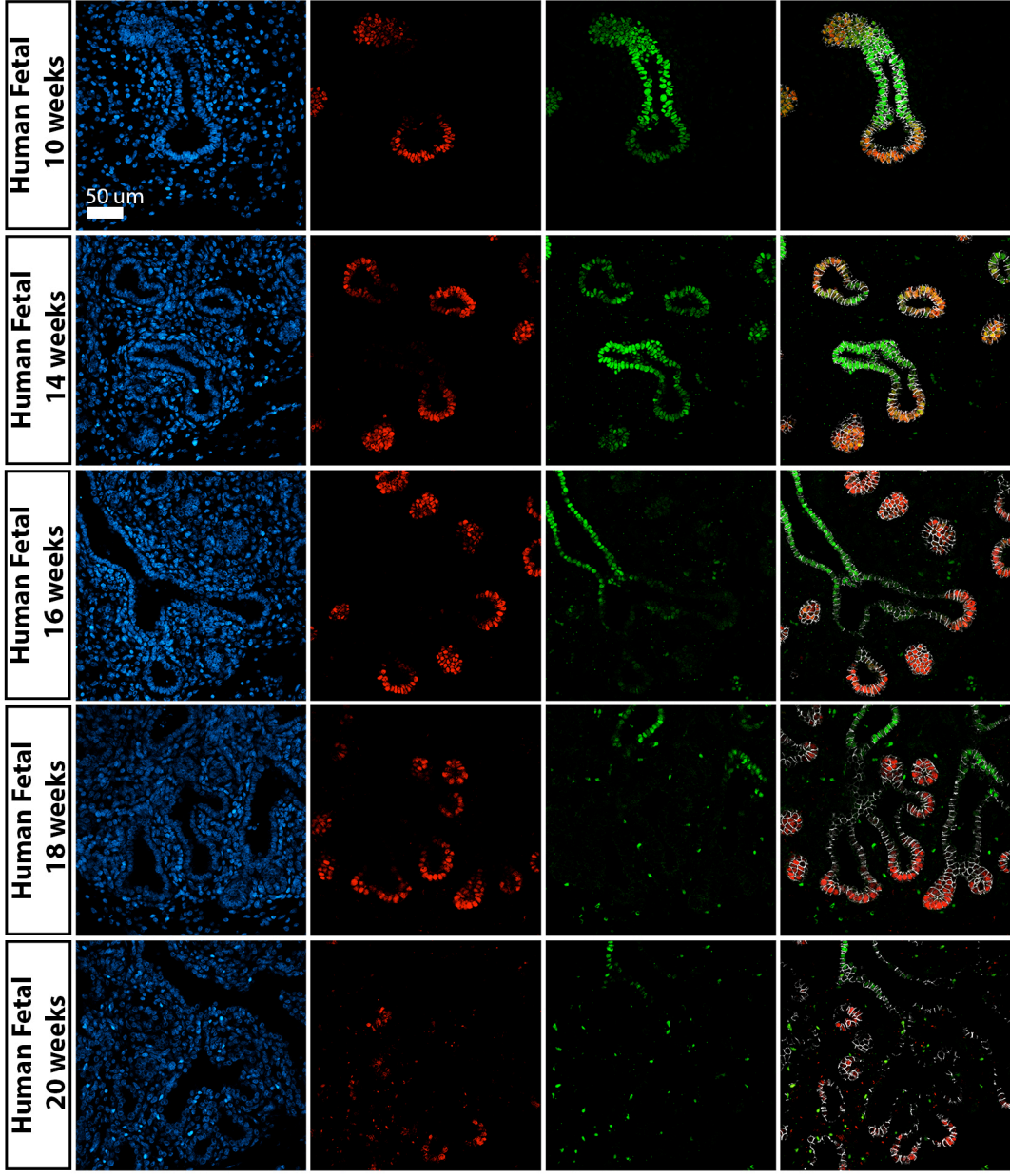
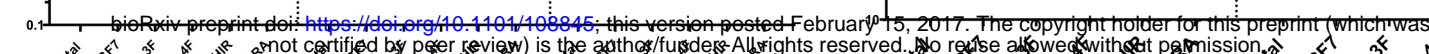


Figure 3





D

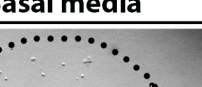
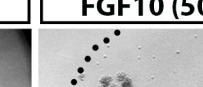
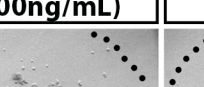
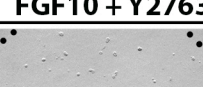
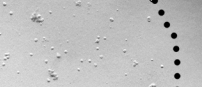
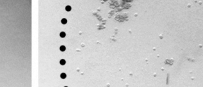
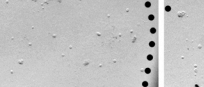
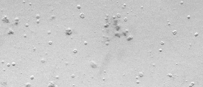
Isolated Human Fetal Distal Lung Buds				
	Basal media	FGF10 (500ng/mL)	FGF10 + Y27632	Y27632
Day 0				
Day 7				

Figure 4

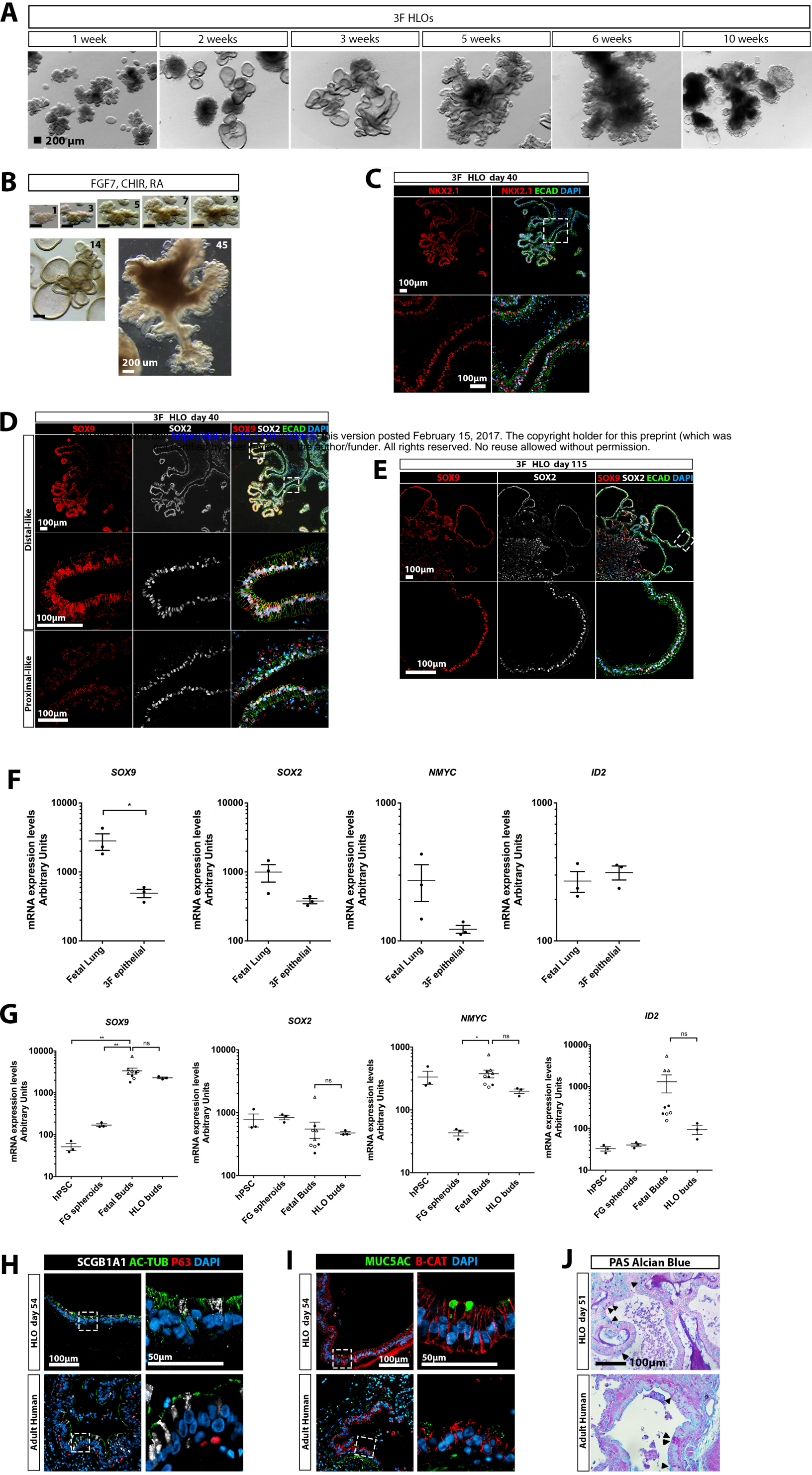


Figure 4, Supplement 1

